Determination residence time distribution of the solid phase in a dry anaerobic semi-continuous horizontal reactor of 0.5 m3 using innovative 3D printed tracers

M.A. Hernandez-Shek, A. Coutu, J. Fayolle, P. Peultier, André Pauss, T. Ribeiro

Determination residence time distribution of the solid phase in a dry anaerobic semi-continuous horizontal reactor of 0.5 m^3 using innovative 3D printed tracers

M.A. Hernandez-Shek[a,b,c,d], A. Coutu[a], J. Fayolle [a,b,c], P. Peultier [c], A. Pauss[b], T. Ribeiro[a*]

[a]Institut Polytechnique UniLaSalle, Université d'Artois, ULR 7519, 19, Rue Pierre Waguet, BP 30313, F-60026 Beauvais Cédex, France.
[b]Université de Technologie de Compiègne, ESCOM, TIMR (Integrated Transformations of Renewable Matter), Centre de recherche Royallieu - CS 60 319, 60 203 Compiègne Cedex, France
[c]Easymetha, 6 rue des Hautes Cornes, 80000 Amiens, France.
[d]Suez Treatment Infrastructure, 16 Place de l'Iris, 92040 Paris La Défense cedex, France

*Corresponding author: Thierry Ribeiro; Tel.: +33 (0) 344 06 76 11; E-mail: **thierry.ribeiro@unilasalle.fr**

Abstract

Solid residence time distribution (SRTD) analysis is important in the design, modeling, and operation of solid biomass in continuous dry anaerobic digestion (D-AD) reactors. SRTD analysis could allow the appropriately adjust of the applicable organic charge and the study of unusable volume due to solid accumulation and preferential pathways. The lack of sustainable, environmentally friendly, and cost-effective solid tracers limits the study of solid flow patterns in D-AD digesters. In this study, 3D printing enabled the fabrication of customized Poly Lactic Acid (PLA) tracers with a specific shape to perform SRTD analysis of the semi-continuous digestion of straw-cattle manure (SCM) in a horizontal reactor of 0.5 m^3. The recovery of tracers at the reactor outlet allowed the determination of the average SRTD at 29.43 days. Solid convection was predominant over diffusion, indicating that the reactor behaves closer to a plug flow reactor (PFR) rather than a complete stirred tank reactor.

Keywords

solid-state anaerobic digestion; pilot scale reactor; straw-cattle manure; biomass valorization; biogas production

1 Introduction

Anaerobic Digestion (AD) process is a microbial process in which organic matter is converted into biomethane by a bacterial consortium in anoxic conditions (van Haandel et Lettinga, 1994). This

process is considered a well-established technology to valorize organic wastes and allows the production of renewable energy in the form of biogas, which is used for power and heat generation. Moreover, the digestate resulting from the process is rich in inorganic compounds and it is used to partially replace chemical fertilizers in agriculture (Mata-Alvarez et al., 2000). AD processes are frequently classified based on the feed stock as wet anaerobic digestion (W-AD) for biomass with less of 15% of Total Solids (TS) and dry anaerobic digestion (D-AD) containing more than 15% of TS content. The principal advantage of D-AD reactors over W-AD is the increase of solid organic content inside the reactors allowing the reduction of volume requirements thereby lower CAPEX and footprint of the process (Karthikeyan et Visvanathan, 2013; Li et al., 2010). Industrial D-AD process can be performed in batch mode and in continuous mode reactors. Batch mode is preferred as it is easier to operate compared to continuous D-AD processes. Among the main limitations of D-AD process operated in batch mode are the unstable biogas production and time-consuming due to its discontinuous loadings and the difficulty to exploit all the biogas produced given the low methane content during the first days of batch duration (André et al., 2018). Because of these disadvantages of D-AD process in batch mode, recently, high interest has been given to horizontal and vertical elongated reactors for the continuous D-AD which can ensure a more regular biogas flow production than batch mode operations due to continuous or semi-continuous feeding. Existing full-scale D-AD processes such as the Kompogas, Laran and Ineval have proved the applicability of continuous D-AD digesters for the treatment of solid wastes (Elsharkawy et al., 2018; Hernandez-Shek et al., 2020; Karthikeyan et Visvanathan, 2013). However, mass transfer limitations at high TS concentrations and high rheological properties (viscosity and yield stress) have been highlighted as critical issues for the design and operation of continuous D-AD reactors (Abbassi-Guendouz et al., 2012; André et al., 2018).

In a D-AD reactor, mass transport is governed by two main mechanisms: diffusion and convection of the liquid and solid phases. According to Bollon et al. (2013), in D-AD the diffusive transport of soluble substrates in the liquid phase is strongly related to the porosity, the viscosity of the medium and the gradient of the concentration. Even if soluble compounds transport mechanisms have been

57 well described for batch and continuous D-AD reactors suggesting the requirement of an optimal
58 mixing or liquid recirculation thought the solid bed to generate an efficient convective soluble mass
59 transport and to provide a good homogenization of soluble compounds (Benbelkacem et al., 2013;
60 Coutu et al., 2022a), a complete description of the mechanisms of solid phase diffusion and
61 convection in D-AD reactors working in continuous have not been completed. Understanding the
62 solid flow behavior and the predominant solid mass transfers D-AD digesters is completely necessary
63 to optimize the design and the operation of continuous D-AD reactors and to develop useful models
64 describing the behavior of biomethane production (Harris et al., 2003). Flow behavior and mass
65 transfers in reactors are often studied by means of a residence time distribution (RTD) analysis. The
66 mean objective of RTD analysis is to measure the probable time that solid or liquid materials would
67 stay inside of continuous flow system processes (Gao et al., 2012). This analysis allows the
68 characterization of the flow profile, the study of non-uniform solid concentration inside the reactor
69 and, the determination of the sliding velocity between the different phases (liquid, gas, and solid).
70 Moreover, the RTD analysis allows to complete the reaction kinetics and to determine the
71 predominant mass transfer between convection and dispersion. In real reactors this information is key
72 to setting the ideal reactor model which would describe better the biological reaction kinetics and the
73 biomethane production from the D-AD digester (Coutu et al., 2022a). Ideal reactors refer to
74 particularly simple configurations, where the hydrodynamic and physical conditions are assumed to
75 be idealized and determined. In practice, this type of reactor does not exist. The ideal continuous
76 reactor models include the ideal complete stirred tank reactor (CSRT) and the ideal Plug Flow Reactor
77 (PFR) (Green et Perry, 2008). While in ideal CSTR homogeneity of mass in the reactor is assumed, in
78 an ideal PFR the substrates and products concentrations are not uniform throughout the reactor length
79 since there is not longitudinal mixing and the mass transfer is governed by convection whereas
80 diffusion does not exist (Stenstrom et Rosso, 2003).

81 The experimental RTD analysis is commonly performed by tracer injection into the reactor inlet and
82 then the tracer concentration is measured in the reactor outlet as a function of time (stimulus -
83 response injection technique) (Fogler, 2006). Considering the high heterogeneity level of the matter

inside a continuous D-AD digester and the presence of a multiphase flow (liquid, gas, and solid), finding the best tracer and detection methods for solid residence time distribution (SRTD) could be a challenging task. According to Green et Perry (2008), a reliable tracer should contain the following characteristics: (1) it must not disturb the flow pattern inside the reactor; (2) it should have physical properties as close as possible to all bulk particle; (3) when more than one phase is involved in the reactor chamber, the tracer must stay in the phase of interest; (4) it must be non-reactive and detectable in small concentrations and (5) the tracer and the detection device preferably should not be too costly. Hitherto, several techniques for solid tracer tests have been developed, each with their advantages and disadvantages. Some methods such as the radioactive tracers, radio frequency identification (RFID) tracers, chemically different tracers and magnetic tracers among others could be cited, however, the discrepancy between the size and the density of the tracers and the bulk particles in the reactors limit the application of the former methods (Buffière et al., 2016; Dehghani Kiadehi et al., 2021). In addition, in addition to the fact that the use of chemical or radioactive tracers could inhibit the functioning of biological reactors, some of these methods are generally expensive, and some of them are constraints of the supply and handling of chemical and radioactive products. These tracers could represent a potential human and environmental risk, besides the disposal of chemical and radioactive waste continues being a limitation for their application in the pilot or real scale processes (Dehghani Kiadehi et al., 2021).

Despite the importance of SRTD analysis on the process D-AD development and optimization, the above-mentioned problems related with the tracer selection argue the limited state-of the art on SRTD analysis on continuous D-AD reactors. To the best of author's knowledge, SRTD analysis has been only performed for the vertical VALORGA digester equipped with biogas stirring and fed with shredded biomass under high digestate recirculation rate (Álvarez et al., 2018; Benbelkacem et al., 2013). Radio-emitting technique was used with spherical solid tracers of different sizes and materials with density between 0.5 and 2.5 g cm^{-3}. In this case, the VALORGA reactor was classified and modeled satisfactorily considered it as a series of ideal CSTRs. Indeed, this digester was fed with shredded biomass and a biogas stirring method allows a certain mixing of the material inside

(Donoso-Bravo et al., 2018). Recently a new type of continuous horizontal reactor has been developed demonstrating the possibility to treat un-shredded biomass in semi-continuous D-AD without no mixing of the solid phase. The D-AD process in this semi-continuous reactor has shown similar physical and rheological changes of the SCM compared to those achieved in batch reactors under the same anaerobic digestion time (Hernandez-Shek et al., 2022). Thus, there are some insights that continuous horizontal D-AD reactors without solid phase stirring and fed with un-shredded biomass could have a closer behavior to a PFR. This hypothesis needs be verified by the realization of a SRTD analysis for a better understanding of this kind of D-AD technology.

The determination of SRTD of continuous D-AD digesters and the impact of different operational parameters over the mass transfer phenomena remain to be further explored. Therefore, this study aims to: (1) determine the SRTD of continuous D-AD reactor treating un-shredded biomass without solid stirring (2) determine the ratio of solid transfer by forced convection and by diffusion, which can give an indication whether the reactor studied is closer to a CSTR or an ideal PFR (3) study the potential of 3D printing applications to fabricate cost effectively and functional solid tracers to perform SRTD in continuous D-AD reactors avoiding the limitations of chemical and radioactive tracers over biological processes. To do so, Poly Lactic Acid (PLA) tracers were printed and applied in a semi-continuous D-AD pilot reactor of 0.5 m^3 treating un-shredded Straw-Cattle Manure (SCM) to determine the SRTD. Different groups of 3D printed tracers were injected mixed with the substrate, the recovery of the tracers in the reactor outlet zone allowed the determination of the average SRTD. Moreover, the Peclet criterion was also determined to classify the predominant displacement of the solid phase between convection or diffusion. Finally, the volumetric evolution of each biomass injection during its transport and digestion was measured by registering the coordinates of each tracer likely an excavation on an archeological site; this analysis enabled the observation of possible solid dead volumes inside the reactor chamber.

2 Materials and Methods

2.1 Substrate and inoculum for continuous D-AD

The SCM used as a substrate was weekly collected from the raked litter material from the livestock barns and the liquid inoculum was obtained from the liquid manure pit from the dairy farm of the Institut Polytechnique UniLaSalle located in Beauvais, France (49°27′58.2″N 2°04′17.5″E). In this farm, non-shredded wheat straw is used as litter material for cows (Prim' Holstein). No conservation of the tested materials was undertaken, they were directly characterized and used in the D-AD reactor. **Table 1** depicts the average values with standard deviation for the physicochemical characterization parameters of the SCM and the inoculum.

2.2 Analytical Methods for Monitoring of AD-D Process

The total solids (TS) and volatile solids (VS) of the raw and digested biomass were determined according to APHA standards (2017). The biochemical methane potential (BMP) of fresh SCM was determined by the traditional incubation method in a AMPTS 1 Device (Automatic Methane Potential Test System, Bioprocess Control, Sweden) following the methodology proposed by Holliger et al. (2016). The pH was determined using a pH meter (Mettler Toledo, Switzerland), the initial pH of the inoculum was 7.71. The buffer capacity (TAC) and the volatile fatty acids (FOS or VFA) concentration were performed by two acidification steps using sulfuric acid in an automatic titrator T50 (Mettler Toledo, Switzerland), the first acidification down to pH 5.0 allowed the TAC to be determined, and the second acidification down to pH 4.4 allowed the quantification of the FOS. The initial FOS/TAC ratio for the inoculum was 0.125.

2.3 Rectangular semi-continuous pilot design

A horizontal reactor (**Fig. 1**) for continuous solid anaerobic digestion process was operated for 147 days (45 days of batch mode and 102 days of continuous feeding). The total reactor volume distributed in three zones (inlet, main and outlet). To ensure the feeding and the matter displacement in the reactor, the inlet zone is provided with an electric piston (MPO-WPC, MotionProPlus, France) with 600 mm of stroke length and a maximal load of 4000 N over a surface of 0.4 x 0.14 m. The main

zone denotes the part of the reactor where biogas is collected, it has 2 meters in length, 0.6 m height and 0.4 m width (480 L of total volume). In this section mesophilic (37 °C) conditions were maintained by recirculating water through a water jacket surrounding the main zone of the reactor with three thermo-regulated baths (Fisherbrand, France) for each part of the three sections of the vessel (see **Fig. 1**). The reactor was shielded with a 40 mm polystyrene surface to limit heat loss. Leachate can be pumped from the liquid stock at the reactor bottom and recirculated to the top of the solid material. Volumetric drum biogas counter (TG 01, Ritter, Germany) was used to measure the biogas production of the reactor. Two ports, one on the liquid circuit and the other on the gas circuit, facilitated the collection of samples for analysis. The composition of the biogas was monitored daily by a gas analyzer (Multitec 540, Sewerin, France). The material was forwarded from the inlet towards the outlet at the end of the reactor by the pressure force applied by the electric linear piston placed in the inlet (**Fig. 1**); as a result, the digested residue was discharged through the outlet while new materials were added. Digestate was manually removed from the outlet while the liquid phase is kept in the reactor to ensure the hydraulic seal and avoid gas leakage.

2.4 3D Tracer development

In this work 20 groups of tracers were printed with a Ultimaker® S5 3D printer using polylactic acid (PLA) of different colors (**Fig. 2**). The mass of each tracer was 3.0 ± 0.1 g and density of 1.25 g/cm^3 (Wu et al., 2022). The tracer's shape was selected in two perpendicularly overlapping crosses creating an isometric 3D, the braces allowed the tracer entanglement with the long lignocellulosic fibers of the SCM, and thus their forwarding from the inlet to the outlet with the digested matter. PLA was chosen because it is as a biodegradable polymer, its density is close to the real density of the wheat straw, 1.18 g/cm^3 (Lam et al., 2008) and the fact that this material cannot be digested at the mesophilic temperature (37 °C) range in which the reactor operated. Besides its reduced cost made PLA interesting for the developed application, indeed, the cost of each tracer was estimated at 0.14 €.

2.5 *Solid residence time distribution (SRTD) analysis*

Solid residence time and particles transport in continuous reactors are usually studied by the construction of RTD curves (Álvarez et al., 2018; Benbelkacem et al., 2013; Jiang et al., 2022). The experimental mean residence time for a pulse injection of tracer can be determined from RTD curves by Eq. (1) and Eq. (2) (Fogler, 2006).

$$E\,(t) = \frac{C(t)}{\int_0^{\infty}(C)dt} \quad \textbf{(1)}$$

$$t_m = \frac{\int_0^{\infty} tE\ (t)dt}{\int_0^{\infty}(E)dt} = \int_0^{\infty} tE\,(t)dt \quad \textbf{(2)}$$

where E(t) is the dimensionless residence-time distribution function, C(t) is the concentration of the tracer at time t, and t_m (s) is the mean residence time. Notice that the former equations will be useful in the case of liquid tracers and allow the experimental determination of the hydraulic retention time considering the relation between the vessel volume and the biomass flow. This determination does not consider the volumetric changes of the solid biomass since the liquid density does not have considerable modifications. Therefore, the solid retention time determination cannot easily be performed by the geometrical relation between the flow and the vessel volume. Moreover, the limited number of solid tracers (20 per injection) made that the concentration of tracers within a sampling volume was therefore not as precise as for the soluble tracers, consequently, Eq. (1) and Eq. (2) cannot be applied directly and the determination of SRTD can be accurately measured by counting the number of tracers extracted from the reactor outlet with the numerical approximation done in Eq. (3) after a given time of the operation (Álvarez et al., 2018; Benbelkacem et al., 2013).

$$N\,(t) = Q\int_0^{t} C(t)dt \sim \sum_{i=0}^{t} N_i \quad \textbf{(3)}$$

where Ni is the number of particles measured at each flush out and t is the number of working days.

The retardation factor (R) describes the ratio between mean residence time and geometrical residence time (Eq. 4). A retardation factor higher than 1 suggests the presence of dead volumes and a retardation factor shorter than 1 suggests the presence of solid phase preferential pathways.

$$R = \frac{\tau}{\tau_G}, \tau_G = \frac{V}{Q} \quad \textbf{(4)}$$

With R the retardation factor (dimensionless), τ the mean residence time (day), τ_G the geometrical residence time (day), and V the volume (m^3).

2.6 One-dimensional dispersion model: Axial dispersion and diffusion analysis

The use of the one-dimensional dispersion model to study axial solids mixing and RTD is frequently used in the study of circulating fluidized bed solid mixing studies. According to Harris et al. (2003), this model represents a simplified manner of describing the previously measured SRTD and it enables the determination of the Peclet criterion or *Bodenstein* number, this is a dimensionless number used to represent the ratio between the total transfer and the transfer by axial diffusion (Grabmüller and Schädlich, 1983; Harris et al., 2003). It could be calculated from SRTD analysis and elution curve variance assuming that convective flow is prevailing on diffusive flow likely an ideal PFR.

This criterion can be interpreted as the relationship between the advective transport rate over the dissuasive transport rate and approximated using method of moments according to Eq. (5):

$$Pe = \frac{advetive\ transport\ rate}{diffusive\ transport\ rate} = \frac{u_p L}{D_{ax}} \sim 2\left(\frac{\tau}{\sigma}\right)^2 \quad \textbf{(5)}$$

Where u_p (m day^{-1}) denotes the known constant fluid velocity down-flowing through the reactor and where L is a characteristic length which in the case of this study was 2 m which corresponds to the reactor vessel length and D_{ax} is the axial dispersion coefficient in $m^2\ day^{-1}$. τ (day) represents the mean residence time and σ the residence time distribution standard deviation (day), calculated as first and second order moments from Eq. (2). The Peclet criterion allows the determination of the predominant displacement of the solid phase between convection or diffusion: if dispersion is much slower than convection, the reactor behaves as though it were in ideal PFR, while if dispersion is very rapid

compared to convection, the reactor approaches a perfect CSTR (Dudukovic et Felder, 1983). Diffusion is said to dominate if Pe is lower than 1. On the other half, the closest Peclet number to 200 indicates that convection would be most important than diffusion, therefore, the kinetic of the solid displacement would be closer to a PFR reactor. D_{ax} is usually determined by the statistical technique knew as the method of moments, this considers the tracer response measured previously in the SRTD analysis by the determination of the variance (σ^2) or usually called the moment of order 2, the variance characterizes the spread of the distribution around the mean residence time (τ) (Dudukovic et Felder, 1983).

2.7 Experimental Set-up

This study has been performed in different phases, each with a different objective **(Fig. 3)**. First, the reactor started-up in batch mode (Patinvoh et al., 2017), followed by the continuous feeding to achieve steady conditions and to verify if tracers let them transport by the solid phase advancement. Then, the SRTD and Peclet number were determined to maintain steady conditions. Finally, the reactor shut down and the three-dimensional analysis of the distribution of the remaining tracers in the reactor.

2.7.1 Phase I: Reactor start up in batch mode

The objectives of this phase were to launch the reactor in batch mode and to evaluate the reactor sealing and the heating, the liquid recirculation, and the biogas monitoring systems. For its realization 80 L of tap water was put into the recirculation stock at the reactor bottom (80 L), then, the SCM was placed on the perforated plaque in layers of 10 cm height and tracers of different colors were well distributed inside the reactor volume (**Fig. 3**). 222.5 kg of fresh SCM (around 36.9 kg of TS) was placed in the reactor with eleven groups of tracers distributed each 20 cm in the reactor length (each group with eighteen tracers for 198 in total). Once the desired volume of SCM was placed (approximately 0.4 m^3 of solid and 10 cm height of headspace gas were kept), the solid was partially immersed into the liquid inoculum until achieving the height of hydraulic sealing in the inlet and outlet of the reactor, to do this, 190 L of inoculum was injected filling the void spaces in the SCM bed. The physicochemical characterization of the inoculum is presented in **Table 1**. Once the reactor

had been filled, this was sealed and heated by the water bath allowing keeping mesophilic temperature (37 °C) during all the experiment duration. During this phase, the reactor operated as a batch LBR and the liquid phase was recirculated and sprinkled over the solid bulk on Monday, Wednesday, and Friday to keep wet the top of the matter and to homogenize the liquid phase (around 40 L). Since no SCM was injected during this period, the tracers initially placed kept their initial position. The D-AD in batch lasted for 48 days until achieving low production of biogas from the batch (<1% of the accumulated volume), during this time the reactor was followed by measuring the biogas flow and composition, the pH, the conductivity, the buffer capacity (TAC) and the volatile fatty acids (FOS).

2.7.2 Phase IIA and IIB: Continuous reactor operation

Once the batch operation ended, the reactor was fed with 33.3 kg of fresh SCM (around 5.5 kg of TS) on Monday, Wednesday, and Friday, getting a load rate of approximately 100 kg $week^{-1}$ or 14.3 kg_{MF} day^{-1}. The continuous operation lasted 85 days and it was divided in two phases (IIA and IIB), the first was used to increase solids content in the reactor (45 days), to achieve steady state and to observe the movement of the initially placed tracers (**Fig. 3**) and the second phase was used to determine the SRTD and to identify the solid diffusion/convection phenomenon behavior using the Peclet criteria, this second phase or continuous feed lasted for 40 days. With every SCM injection of the reactor matter inside was pushed and forwarded until the reactor outlet. During the continuous operation, the produced gas and the liquid phase were monitored with the same parameters used for the batch mode process following.

2.7.3 Phase III: Reactor shut down and spatial evolution analysis of tracers inside the reactor

Once the SRTD analysis was carried out, the reactor was opened, and solid surface shape was topographically surveyed using a laser distance meter JX-50M with accuracy of 1 mm (Crafton, France). Then, the solid was removed layer by layer and the X, Y, Z coordinates of each 3D printing solid tracer were located like an excavation on an archeological site using the laser distance (**Fig. 3**). Blender® software was used to create a 3D representation of the distribution of the tracers inside the reactor. This analysis enabled the observation of the volumetric evolution of each biomass injection

inside the reactor and to fully describe the solid flow pattern and the possible presence of "dead" volumes inside the reactor chamber.

3 Results and discussion

3.1 Increase of solid content in the reactor and establishment of steady conditions

The PFR was operated in batch mode for 48 days after the reactor launching. During this time, biogas flow and composition and liquid analysis were monitored (section 3.5). The results of this batch monitoring (the specific biogas flow, the biogas composition and the pH, conductivity, VFA and alkalinity of the liquid phase) presented similar behavior to the 60 L batch D-AD digesters treating SCM presented by Hernandez-Shek et al. (2020). Once the biogas production of the batch was inferior to 1% of the cumulated biogas volume, the reactor was continuously fed. The Inlet and outlet behavior during continuous operation (IIA and IIB) is depicted in **Fig. 4.** Notice that in the first 33 days of the continuous cycle IIA, the outlet was principally the liquid phase initially injected and solid content inside the reactor increased until it started pushed and compressed by itself; likely a toothpaste tube in which the material is pressed from one side, and it flows by the action of the piston effect. Similar observation was made by Hernandez-Shek et al. (2022) with a lower load rate than the one used in this work. During the first cycle of continuous feeding the ratio between the solid inlet and the outlet was stabilized and the digestate of the initial SCM used for the batch test was completely flushed out. This fact was corroborated by the progressive recovery in the outlet of all the initial tracers evenly placed in the solid bed volume. The first experiment under continuous feeding demonstrated that the selected shape of the tracers allowed satisfactorily their entanglement and transport with the solid biomass limiting their settlement or their flotation. The recovery at the reactor outlet of the initially evenly placed tracers according to the number of injections is shown in **Fig. 5a**. Under continuous operation, 21 injections were necessary to completely flush out the digested SCM placed in phase I. Moreover, PLA resulted in a suitable material for the tracer fabrication and supported the mesophilic temperature range adequately. According to Bernat et al. (2021), PLA is anaerobically biodegradable under certain conditions at temperatures of the order of 60 °C, as

304 consequence, it is not recommended perform SRTD on D-AD reactors working at the thermophilic
305 temperature range (55 - 60°C).

306 An average elution RTD curve of the recovery at the outlet of the 11 groups of evenly placed tracers
307 is shown in **Fig. 5b.** Most of the RTD curves exhibited a single distinct peak. Considering the high
308 standard deviation and the non-uniform way that the evenly placed tracers of each group were
309 recovered, it was observed that the horizontal displacement of the solid matter was not uniform in the
310 cross plane of the solid bed. This suggests that the shear force applied in the inlet would not be
311 transferred in a uniform manner to the solid bed axial surface. Consequently, there are some
312 horizontal layers that would be easier displaced towards the reactor outlet than others affecting the
313 overall solid displacement and therefore the solid residence time. Unfortunately, not specific marks
314 indicating the initial height were made to tracers initially placed at different positions of the solid bed
315 to corroborate this fact. This action could have been useful to determine the layers with the grandest
316 and lowest motion. A positive observation was the fact that all the tracers initially inserted into the
317 solid bed were recovered at the reactor outlet, indicating that sooner or later almost all the initial
318 biomass used for the batch reactor start-up would be flushed from the pilot reactor as digestate. If this
319 experiment can be performed in a larger reactor treating non-shredded SCM obtaining the same
320 results, it means that this kind of reactor would have a very valuable asset compared to others pilot
321 and industrial D-AD reactors not only by avoiding the use of size reduction processes and their costs
322 involved, but also by avoiding the use of mechanical parts inside the reactor to ensure the solid bed
323 forwarding as in the case of the reactors used in recent studies such as those performed by Arias et al.
324 (2021), Chinellato et al.(2021), Kim et Oh (2011), Patinvoh et al. (2017), Rasouli et al. (2018) and
325 Veluchamy et al. (2019).

326 **Fig. 5c** depicts an attempt to determine the number of injections required to flush out every single
327 group of tracers initially positioned in the solid bed. For example, to fully recover the group of tracers
328 initially positioned at 0.2 m to the outlet (yellow tracers), around 5.2 injections were required. Please
329 note that the solid advancement in the reactor was not linear; instead, it can be observed that tracers
330 initially placed between 0.60 and 1.4 m from the outlet presented a slowdown. This reduction in the

solid advancement is explained by the increase of the solid content and the compression of the solid inside the reactor which would reduce the presence of short circuits and reduce the solid quantity of movement. Moreover, this argues the detriment of the liquid fraction while the solid phase increases it concentration (**Fig. 4**). Water distribution in the solid bed has been already satisfactory measured in batch D-AD systems by tomography techniques (André et al., 2015; Degueurce et al., 2016) and water curve methods (Garcia-Bernet et al., 2011a; Hernandez-Shek et al., 2020). Since water content is an important parameter to enhance biological degradation and to limit the rheological constrains of the solid media; a deeper study on the physical changes of the solid bed while the reactor is operated in continuous mode would be necessary to give better comprehension of the liquid loss due to the solid bed macro-porosity loss given the solid compaction.

3.2 Solid residence time distribution analysis and mass transfers characterization

Once all the tracers from the previous phase were recovered and the reactor achieved steady conditions remarked by the stabilization of the ratio between the inlet and the outlet (**Fig. 4**), the steady biogas flow (**Fig. 9b**) and the regularity of the liquid monitored parameters (pH, conductivity, VFA and Alkalinity), the second part of this study concerned the experimental determination of the SRTD in the reactor at the selected feeding conditions. In this case, the reactor was fed with a mixture of SCM and 20 solid tracers (**Fig. 3** – IIB), 3 tracers were placed in the reactor inlet width every time that the piston pushed injecting the biomass into the reactor. Several injections were required to forward the mass from the inlet to the outlet and once 4 groups of tracers were recovered at the outlet, different RTD curves were designed to measure the average time of residence of solid matter inside the reactor (**Fig. 6**). The average elution curve depicted in **Fig. 6** differs in the spread of the response peak about the mean (σ) from those presented by Benbelkacem et al. (2013) for the SRTD analysis in the VALOGA digester. This suggests that the value of σ was lower for the studied reactor than for the referred one, obtaining a narrower peak and more uniform peak being these characteristics of real PFR reactors (Dudukovic et Felder, 1983). Additionally, comparing the RTD curves depicted in **Fig. 5b** and **Fig. 6** for phases IIA and IIB respectively, it can be noticed that the dimensionless time of section IIA was in total around 8 whereas for phase IIB this value was between 3 and 4. Also the t_{peak}

of the RTD curve was present at 2 for section IIA and at 1 for section IIB. These facts prove that the group of tracers evenly placed took more time to flush out from the reactor than those from section IIB corroborating the impact short-circuit and the exceed of free water over the residence time once continuous operation started. Under the operation conditions selected for this work; the average injection frequency was 2.29 days and the average solid displacement in steady state was 6.61 ± 0.23 cm/day. The average SRT was calculated at 29.43 ± 1.05 days a geometric residence time of 30.25 days, a retardation factor (R) described by Eq. 4 of 0.97. This difference suggests the possible presence of "solid dead" volumes or zones of low transit of solids inside the reactor, these which would be further discussed in the next section.

In this work the focus of attention was the study of the transport mechanisms (diffusion and convection) of the solid phase which could be even more strongly limited than solved compounds in the liquid phase given the rheological properties of the solid medium. Using **Eq. 5** and based on the SRTD results, the dimensionless Peclet number was computed at 128.6, according to Dudukovic et Felder (1983), when Peclet number approaches 0 means that the reactor functioning would be closer to an ideal CSTR and diffusion is predominant over convection, whereas if this number is tends to 200, convection is stronger and ideal PFR approach can be useful to describe the reactor working. The solid axial diffusion (D_{ax}) was determined at 0.132 m^2 day^{-1}, this is a very low value of diffusivity for the solid phase in the reactor compared with the axial diffusion coefficient of liquids which has increased with the liquid velocity from 21 to 276 m^2 day^{-1} (Moreau et al., 2017). The diffusive flux is related to the gradient of the concentration of solids in the reactor, this could mean that the concentration of TS was somewhat homogeneous through the reactor length. Unfortunately, although the TS content was measured in section 3.3 for the determination of VS destruction (**Fig. 7c**), the sampling process allows the release of free water from the solid, thus the measured TS content (data not shown) does not correspond exactly to the operational conditions in the reactor enhanced by the solid immersion in the liquid phase. Thus, water content measured in samples correspond mostly to capillary and bound water (Garcia-Bernet et al., 2011a; Hernandez-Shek et al., 2020).

The high value of Peclet number and the low value of solid axial diffusion demonstrate that the overall solid displacement in the designed D-AD continuous digester behaves more like a piston rather than a perfectly agitated reactor. This particularity of this continuous D-AD digester treating un-shredded SCM and devoid of mechanical or biogas stirring corroborates the hypothesis developed by Hernandez-Shek et al. (2022) in which the solid degradation of each injection of un-shredded biomass in the designed reactor could be considered as a plug (a separate entity or an infinitesimally small batch reactor inside the continuous reactor volume). Regarding the load rate and the operational characteristics, each injection of 33.3 kg of SCM could be considered as the launch of a new batch digester and the working reactor volume could represent the equivalent of 13.2 batches launched one after the other with a retention time of 29.43 days each. This condition differs from the results of the RTD analysis of the VALORGA reactor which was described and modeled as a series of CSTR, differences between these reactors are mainly explained by the use of shredded biomass and the presence or gas stirred in the case of the VALORGA system used by Álvarez et al. (2018) and Benbelkacem et al. (2013a) that would increase the diffusion mass transfers. Noting the specific reactor behavior observed in this work, the next step could be the development of a simplified model using batch data to estimate the biogas flow from this kind of D-AD reactor. Additional work is ongoing based on the use of AM2 model (Coutu et al., 2022b) and the results of this study.

3.3 Three-dimensional analysis of the spatial evolution of tracers inside the reactor

The final part of this work was to study the dispersion of the tracers inside the reactor. The objective was to go deeper in the comprehension of the solid evolution of a reactor devoid with mechanical parts in the interior to ensure mixing or solid displacement. Once the SRTD analysis was achieved, the reactor was opened, and solid surface shape was topographically surveyed **(Fig. 7a)**, the resulted solid surface was not uniform and a reduction of around 50% of the initial headspace gas was observed. Then, the solid was removed by layers and the X, Y, Z coordinates of each 3D printing solid tracer were surveyed. The distribution of each injection in the reactor with the selected operational conditions is depicted in **Fig. 7b**. This analysis confirmed that the solid was not evenly distributed, thus, the biodegradation performance is not constant along the distance in the reactor, this

411 fact will be further discussed in the next section of this work based on the results of VS destruction.
412 From **Fig. 7b**, notice that the injection arranged sometimes one over the other likely the movement of
413 tectonic plates, moreover, there is not an axial mixing between the solid injections, instead each of
414 them is forwarded by the action of the push effect given by piston force in the inlet and the
415 rheological changes of the solid phase while this is biodegraded (Garcia-Bernet et al., 2011b;
416 Hernandez-Shek et al., 2022, 2021).

417 The change in volume that each injection would experiment through its displacement can be observed
418 in **Fig. 7b** and the calculated volumes of each injection are in **Fig. 7d**. Considering the initial volume
419 of the injection inside the reactor (around 37 L) and the last injection before the outlet, this value
420 could decrease between 42 and 74%. The volumetric reduction of biomass is explained by the
421 compaction force of the piston and the physical breakdown of the lignocellulosic fibers that would
422 reduce the bulk density, the macropores and the rheological properties of the solid biomass
423 (Hernandez-Shek et al., 2022, 2020). The volumetric reduction of solid and non-shredded biomass
424 treated in a PFR indicates that the ratio between the organic load rate and the solid retention time is
425 not linear like in a PFR in which the inlet and the outlet have similar density and both are generally in
426 liquid state. Moreover, the presence of « dead » volumes can also be observed in the upper part of the
427 solid bulk (**Fig. 7b)**. In this zone liquid phase was highly present that solid, this could be explained
428 since the displacement of the matter may be faster in the bottom of the reactor than in the upper zone.
429 The geometrical shape of the inlet and the applied force downward of the piston enhance liquid
430 impregnation of the solid phase with the liquid present in the reactor vessel, however, it could also
431 enhance solid compaction in the deepest zone reducing the free water placed in the macropores of the
432 solid bed.

433 The three-dimensional analysis of the spatial evolution of tracers inside the reactor suggests that to
434 ensure semi-continuous D-AD reactors the operation and to improve their methane production,
435 several strategies for controlling the presence of water inside the reactor could be used; the first
436 strategy could be the reduction of the solid load rate, this could improve mass transfers between the
437 solid and the liquid phases by increasing the SRT inside the reactor vessel and achieving a higher

reduction of the rheological properties of the substrate and higher recovery of the BMP. The second strategy concerns the solid immersion which has resulted a good strategy to ensure the hydraulic sealing of the reactor inlet and outlet; additionally, it could also facilitate the horizontal displacement of the matter inside the reactor by reducing the apparent rheological properties. Another strategy could be to apply solid digestate recirculation to reduce the physical and rheological differences between the inlet and the outlet, improving the flowability of the biomass. However, the impact on biogas production of this strategy for the designed rector needs to be studied. Finally, considering the results of SRTD and the traces distribution in the reactor different geometry ratios (width, height and length) or feeding systems (i.e. screw feeder, piston feeder and pocket feeder) could be designed to optimize the semi-continuous D-AD reactor performance and reduce as much as possible the presence of dead volume in the reactor (Brambilla et al., 2013).

3.4 Potential applications and possible drawbacks of 3D tracers for SRTD determination and D-AD

3D printers allow the simple fabrication of tracers and solid parts with customized shape and size, and the desired surface and porosity. Several materials can be used in 3D printers (plastics, resins, polyamide, metals, and ceramics) each with different mechanical properties that could easily emulate the properties of the solids phase on which SRTD analysis in required. Among all these materials, in this study the PLA was founded as a convenient material to create solid tracers for the determination of SRTD in a semi-continuous D-AD digester treating un-shredded SCM. The solid tracers developed were cost effective, environmentally friendly, and the production cost of the total number of tracers used in this work was around 75€ (0.14 € each) which is very inexpensive compared with other SRTD techniques such as RFID technique (Radio Frequency IDentification) which each tag may cost between 10 and 15 €, or the radioactive and magnetic tracers its price can easily exceed several thousand euros just for their installation and use, without including the price of waste disposal and management (Benbelkacem et al., 2013; Dehghani Kiadehi et al., 2021). The density of PLA was satisfactory to avoid the settlement and flotation of the tracers compared with other materials such as glass used by Benbelkacem et al. (2013) having a density of 2.5 g cm^{-3} or the polypropylene with 0.9

465 g cm^{-3}. The PLA did not show beneficial or antagonistic effect on biogas production by the tracer's
466 presence since no inhibition or higher biogas production was observed.

467 Tracers were placed in the inlet zone with enough space to avoid physical interactions with each
468 other, indeed, the friction between tracers could eventually give high structuration to the matter and
469 play a reverse effect in its rheological properties and flowability. In this work the definition of the
470 optimal number of tracers per injection was not defined and was arbitrarily selected by the authors.
471 Considering that 20 tracers of 3 g each (60 g in total) were mixed with 33.3 kg of SCM for each
472 injection, the mass of tracers represents less than 0.001% of the injected mass and each tracer may
473 represent the flow of around 1.6 kg of SCM. Based on the very low mass and volume ratios between
474 the tracers and the SCM, the number of used tracers and their presence in the solid would not have a
475 significative impact over the mass transfer and the rheological properties in the reactor since these
476 were easily integrated and forwarded by the SCM in the reactor. However, even if the effect of the
477 tracer's presence was judged low it would be necessary to measure it. Unfortunately, in this study it
478 was not possible to perform this analysis, a possible way could be to measure the force required by the
479 piston injector in the inlet to inject the biomass with and without solid tracers. Other options are to
480 use rheological tools to fully describe the effect of the number, shape of solid tracers over the
481 rheological properties of the biomass. So far, no study has been found in literature on the optimal
482 number of solid tracers to use to avoid significant changes in the physical or rheological properties of
483 the solid phase.

484 Deformation and breaking of some tracers were observed during the three-dimensional analysis
485 described in Section 3.3. Indeed, the temperature effect combined with the shear force would bend or
486 break some of the tracers. A careful analysis of PLA deformation would also allow the
487 characterization of the deformation forces applied over the biomass to ensure their displacement
488 inside the PFR and complete the rheological information of solid biomass provided by Hernandez et
489 al (2022). Moreover, this analysis could enable the optimization of shape and size for future 3D
490 printed tracers used in SRTD determination in continuous D-AD reactors and other chemical process
491 involving the biomass transformation. Finally, the main limitation of using the developed PLA tracers

is the manual detection which could limit their use in D-AD digesters bigger than that one used in this work. Further work could be performed to identity the optimal number of tracers to use in SRTD based on the different substrates used in D-AD and to test other tracer's shapes (i.e spheric, cubic or other) and to design a simple and reliable tracers detection system.

3.5 AD reactor performance: Biogas production and solid degradation

Contrasting the semi-continuous D-AD reactor performance used in this work with other studies present in the literature, the following results could argue that the presence of the solid tracers for SRTD analysis did not impact the reactor performance for solid degradation of SCM and the biogas production. Solid samples were taken from different positions in the reactor length and the VS consumption using load rates of 14.3 kg $_{FM}$ SCM day^{-1} compared with the 9.9 kg SCM day^{-1} used by Hernandez-Shek et al. (2022); the results of VS evolution are depicted in **Fig. 7c**. In this work was determined as 29.43 days with 14.3 kg $_{FM}$ day^{-1} of load rate, thus it is expected that for 9.9 kg SCM day^{-1} of load input, the solid retention time in the digester could be around 42.2 days, thus better degradation of VS using a lower load rate, but less biogas produced per digester volume. **Fig. 7c** indicated that the studied reactor had a lower performance (e.g., VS from 81.34 % to 75.1%) than the referred reactor (e.g., VS from 85.8 % to 73.2%). Suggesting that 42.2 days of SRT enable higher methane recovery and VS destruction than the SRT used in this work that was around 30 days. From **Fig. 7c** it can also be observed that solid anaerobic degradation was not constant along the distance in the PFR using 14.3 kg $_{FM}$ SCM day^{-1} and the good linear correlation (R^2 = 0.97) obtained by Hernandez-Shek et al. (2022) indicated a more homogeneous effective volume distribution using a lower load rate. It can be observed that at 1.0, 1.70 and 2.0 meters the standard deviation was higher than other points, considering the **Fig. 7b**, these discrepancies in solid degradation are mainly due to the fact the sampled points in the same section might have solid mass from different injections and therefore different retention time in the reactor.

The overall biogas flow in this study is depicted in **Fig. 8a**. In the first part of the work, the reactor was started up in batch, notice that biogas flow conserves the same appearance as other studies in the literature using SCM as substrate (Hernandez-Shek et al., 2020). During the batch mode operation, the

519 presence of peaks of methane production is observable at days 12 and 19 respectively. Batch mode
520 was maintained for 48 days, the continuous feeding allows to increase the biogas flow until achieving
521 steady state of day 93. The decrease in biogas flow on days 63 and 86 is explained by an accidental
522 shutdown of the heating baths; however, the reactor performance was promptly recovered after a few
523 days. **Fig. 8b** depicts the evolution of methane content in the biogas, this was around 55.1 ± 3.0% in
524 the continuous operation during steady state; this value was the same achieved by Dong et al. (2019)
525 treating cattle manure in a large scale PFR and lower compared with the continuous D-AD reactor
526 developed by Patinvoh et al. (2017) which obtained values around 64 % of methane using anaerobic
527 sludge as inoculum. **Table 2** summarizes the experimental conditions and the experimental results of
528 the continuous operation (II B). In this work the organic load rate (OLR) was calculated at 5.1 g_{VS}
529 day^{-1} $L^{-1}_{reactor\ volume}$ and the specific methane yield was 179 ± 9 NL CH_4 kg_{VS}^{-1}, this value was slightly
530 higher to 146 ± 10 NL CH_4 kg_{VS}^{-1} presented by Patinvoh et al. (2017) for OLR of 6.0 g_{VS} day^{-1} $L^{-1}_{reactor}$
531 $_{volume}$. This difference of around 18 % in methane yield recovery from SCM could be explained by the
532 positive effects of the liquid strategies management applied in this study.

533 The cumulated methane production (**Fig. 8c**) shows a stable production of biogas using a feed rate of
534 14.3 kg $_{FM}$ day^{-1}, in contrast to Hernandez et al. 2022 using a feed rate of 9.9 kg $_{FM}$ day^{-1} the slope of
535 the cumulated was 0.48 compared with 0.63 achieved in this work. This indicates that increasing from
536 9.9 to 14.3 kg $_{FM}$ day^{-1} (around 30%) the load rate of the reactor, the produced volume of biogas per
537 volume unit of the reactor would be increased from 26.5 Nm^3 CH_4 per m^{-3} of digester working volume
538 per day until 32.9 Nm^3 CH_4 m^{-3} day^{-1}. However, as established before, using a lower load rate will
539 allow to achieve better biomethane potential (BMP) recovery for each kg of fresh SCM injected in the
540 reactor. From **Table 2,** the BMP recovery using 14.3 kg $_{FM}$ day^{-1} was 78.2 % while using 9.9 kg $_{FM}$
541 day^{-1} allowed the recovery of around 86.8 % of BMP recovery. Finally, the liquid monitoring by the
542 pH, the conductivity, the AGV production and the buffer capacity; these parameters remained almost
543 invariable over the continuous operation. These results suggest that combined immersion with liquid
544 recirculation is a good strategy to avoid process inhibition, ensure solid degradation in D-AD and
545 biomethane production at the load rate used in this work. Moreover, during the continuous

546 experimentation liquid inoculum injection was done just to keep the hydraulic sealing, thus, it is
547 possible and agreeing with Dong et al. (2019) that the abundance of lignocellulose decomposing
548 bacteria (*Bacteroidete, Firmicutes, Cloacimonetes,Fibrobacteres*) and methaneforming
549 *Methanosarcina* and *Bathyarchaeota* might have been enriched during the continuous reactor
550 operation.

551 **4 Conclusions**

552 The use of 3D printing to create customized shape, size and material tracers have been studied. The
553 solid tracers developed in this work were cheap and environmentally friendly compared with other
554 SRTD techniques. The density of PLA was satisfactory to avoid the settlement and flotation of the
555 tracers. The shape of tracers in two perpendicularly overlapping crosses enable their entanglement
556 with the long fibers of the SCM used as the substrate and allowing the determination of the SRTD in
557 the PFR at 29.43 days using 14.3 kg $_{FM}$ day^{-1} as the load rate.

558 The SRTD analysis results allow us to fully describe the flow patterns of the solid phase in the reactor
559 and its volumetric change caused by the solid degradation and the compaction force applied by the
560 piston. Axial dispersion and diffusion analysis were important to determine the movement of the solid
561 phase is closer to an ideal PFR in which the convection movement was superior to diffusion. This
562 suggests that the biogas flow of the PFR could be modeled considering each injection as the launch of
563 a batch reactor inside the continuous reactor. This condition could be useful to predict the biogas
564 production of continuous D-AD digesters operated without un-shredded substrates and devoid of
565 mechanical parts inside the reactor to ensure solid matter forwarding and mixing.

566 Given the physical changes and the solid fiber degradation of the solid biomass threaded in a
567 continuous D-AD reactor, the solid bulk volume could be reduced from around 42 to 74%. The
568 volumetric reduction of solid and non-shredded biomass treated in a PFR suggests that the ratio
569 between the organic load rate and the solid retention time is not linear as in a PFR in which the inlet
570 and the outlet present similar density and are generally in a liquid state. The change of substrate
571 volume needs to be considered for a better modeling of continuous D-AD reactors.

5 Acknowledgments

The authors wish to thank the Association Nationale de la Recherche et de la Technologie (ANRT) for the financial support of this work, for the Ph.D. grant of Manuel HERNANDEZ-SHEK (CIFRE n° 2017/0352) and for the Ph.D. grant of Joseph FAYOLLE (CIFRE n°2020/1393). The authors would like to thank the GeoLab of UniLaSalle for their support in the 3D printing of the solid plotters used in this work. A special thanks to Raphael Olivier for the visual representation of tracer distribution inside the reactor.

6 References

Abbassi-Guendouz, A., Brockmann, D., Trably, E., Dumas, C., Delgenès, J.-P., Steyer, J.-P., Escudié, R., 2012. Total solids content drives high solid anaerobic digestion via mass transfer limitation. Bioresour. Technol. 111, 55-61. https://doi.org/10.1016/j.biortech.2012.01.174

Álvarez, C., Colón, J., Lópes, A.C., Fernández-Polanco, M., Benbelkacem, H., Buffière, P., 2018. Hydrodynamics of high solids anaerobic reactor: Characterization of solid segregation and liquid mixing pattern in a pilot plant VALORGA facility under different reactor geometry. Waste Manag. 76, 306-314. https://doi.org/10.1016/j.wasman.2018.02.053

André, L., Lamy, E., Lutz, P., Pernier, M., Lespinard, O., Pauss, A., Ribeiro, T., 2015. Electrical resistivity tomography to quantify in situ liquid content in a full-scale dry anaerobic digestion reactor. Bioresour. Technol. 201, 89-96. https://doi.org/10.1016/j.biortech.2015.11.033

André, L., Pauss, A., Ribeiro, T., 2018. Solid anaerobic digestion: State-of-art, scientific and technological hurdles. Bioresour. Technol. 247, 1027-1037. https://doi.org/10.1016/j.biortech.2017.09.003

APHA, 2017. Standard methods for the examination of water and wastewater, 23^{e} ed, American Public Health Association. Inc. Washington, DC.

Arias, D.E., Veluchamy, C., Habash, M.B., Gilroyed, B.H., 2021. Biogas production, waste stabilization efficiency, and hygienization potential of a mesophilic anaerobic plug flow reactor processing swine manure and corn stover. J. Environ. Manage. 284, 112027. https://doi.org/10.1016/j.jenvman.2021.112027

Benbelkacem, H., Garcia-Bernet, D., Bollon, J., Loisel, D., Bayard, R., Steyer, J.P., Gourdon, R., Buffière, P., Escudié, R., 2013. Liquid mixing and solid segregation in high-solid anaerobic digesters. Bioresour. Technol. 147, 387-394. https://doi.org/10.1016/j.biortech.2013.08.027

Bernat, K., Kulikowska, D., Wojnowska-Baryła, I., Zaborowska, M., Pasieczna-Patkowska, S., 2021. Thermophilic and mesophilic biogas production from PLA-based materials: Possibilities and limitations.

602 Waste Manag. 119, 295-305. https://doi.org/10.1016/j.wasman.2020.10.006

603 Bollon, J., Benbelkacem, H., My Gourdon, R., Buffi, P., 2013. Measurement of diffusion coefficients in dry
604 anaerobic digestion media. https://doi.org/10.1016/j.ces.2012.11.036

605 Brambilla, M., Romano, E., Cutini, M., Pari, L., Bisaglia, C., 2013. Rheological properties of manure/biomass
606 mixtures and pumping strategies to improve ingestate formulation. Am. Soc. Agric. Biol. Eng. 56,
607 1905-1920.

608 Buffière, P., Escudie, R., Benbelkacem, H., 2016. Assessment of solid mixing characteristics through tracer tests
609 using radio-frequency identification (RFID), in: 6th International Conference on Engineering for Waste
610 and Biomass Valorisation -May 23–26, 2016 – Albi, France. p. 205.

611 Chinellato, G., Battista, F., Bolzonella, D., Cavinato, C., 2021. Single-phase anaerobic digestion of the organic
612 fraction of municipal solid waste without dilution: Reactor stability and process performance of small,
613 decentralised plants. https://doi.org/10.1016/j.wasman.2021.02.009

614 Coutu, A., André, L., Guérin, S., Rocher, V., Pauss, A., Ribeiro, T., 2022a. Transport and retention modeling of
615 the liquid phase through a stratified porous leach-bed. Application for solid-state anaerobic co-digestion of
616 cattle manure and roadside grass. Bioresour. Technol. Reports 18, 101114.
617 https://doi.org/10.1016/J.BITEB.2022.101114

618 Coutu, A., Hernández-Shek, M.A., Mottelet, S., Guérin, S., Rocher, V., Pauss, A., Ribeiro, T., 2022b. A
619 coupling model for solid-state anaerobic digestion in leach-bed reactors: Mobile-Immobile water and
620 anaerobic digestion model. Bioresour. Technol. Reports 17, 100961.
621 https://doi.org/10.1016/J.BITEB.2022.100961

622 Degueurce, A., Clément, R., Moreau, S., Peu, P., 2016. On the value of electrical resistivity tomography for
623 monitoring leachate injection in solid state anaerobic digestion plants at farm scale. Waste Manag. 56,
624 125-136. https://doi.org/10.1016/j.wasman.2016.06.028

625 Dehghani Kiadehi, A., Leturia, M., Otaola, F., Ould-Dris, A., Saleh, K., 2021. A novel technique for residence
626 time distribution (RTD) measurements in solids unit operations. Adv. Powder Technol. 32, 611-618.
627 https://doi.org/10.1016/J.APT.2021.01.006

628 Dong, L., Cao, G., Guo, X., Liu, T., Wu, J., Ren, N., 2019. Efficient biogas production from cattle manure in a
629 plug flow reactor: A large scale long term study. Bioresour. Technol. 278, 450-455.
630 https://doi.org/10.1016/j.biortech.2019.01.100

631 Donoso-Bravo, A., Sadino-Riquelme, C., Gómez, D., Segura, C., Valdebenito, E., Hansen, F., 2018. Modelling
632 of an anaerobic plug-flow reactor. Process analysis and evaluation approaches with non-ideal mixing
633 considerations. Bioresour. Technol. 260, 95-104. https://doi.org/10.1016/j.biortech.2018.03.082

634 Dudukovic, M.P., Felder, R.M., 1983. Dispersion Model., in: Mixing Effects in Chemical Reactors. American

635 Institute od Chemical Engineers, Washington, p. 39-49.

636 Elsharkawy, K., Elsamadony, M., Afify, H., 2018. Comparative analysis of common full scale reactors for dry
637 anaerobic digestion process. E3S Web Conf. 8. https://doi.org/10.1051/e3sconf/20198301011

638 Fogler, H.S., 2006. Distributions of residence times for chemical reactors. Elem. Chem. React. Eng. 867-944.

639 Gao, Y., Muzzio, F.J., Ierapetritou, M.G., 2012. A review of the Residence Time Distribution (RTD)
640 applications in solid unit operations. Powder Technol. 228, 416-423.
641 https://doi.org/10.1016/J.POWTEC.2012.05.060

642 Garcia-Bernet, D., Buffière, P., Latrille, E., Steyer, J.P., Escudié, R., 2011a. Water distribution in biowastes and
643 digestates of dry anaerobic digestion technology. Chem. Eng. J. 172, 924-928.
644 https://doi.org/10.1016/j.cej.2011.07.003

645 Garcia-Bernet, D., Loisel, D., Guizard, G., Buffière, P., Steyer, J.P., Escudié, R., 2011b. Rapid measurement of
646 the yield stress of anaerobically-digested solid waste using slump tests. Waste Manag. 31, 631-635.
647 https://doi.org/10.1016/j.wasman.2010.12.013

648 Grabmüller, H., Schädlich, H.K., 1983. Residence time distribution of plug flow in a finite packed-bed chemical
649 reactor. Chem. Eng. Sci. 38, 1543-1553. https://doi.org/10.1016/0009-2509(83)80090-6

650 Green, D.W., Perry, R.., 2008. Residence Time Distribution and Mixing, in: Chemical Engineers' Handbook - 8
651 Edition. Professional McGraw-Hill.

652 Harris, A.T., Davidson, J.F., Thorpe, R.B., 2003. Particle residence time distributions in circulating fluidised
653 beds. Chem. Eng. Sci. 58, 2181-2202. https://doi.org/10.1016/S0009-2509(03)00082-4

654 Hernandez-Shek, M.A., André, L., Peultier, P., Ribeiro, T., Pauss, A., 2021. Immersion Effect on the Anaerobic
655 Degradation and the Rheological Properties of Straw - Cattle Manure (SCM) at 440 L Batch Pilot Scale
656 Reactor. Waste and Biomass Valorization. https://doi.org/10.1007/s12649-021-01458-2

657 Hernandez-Shek, M.A., Mathieux, M., André, L., Peultier, P., Pauss, A., Ribeiro, T., 2020. Quantifying porosity
658 changes in solid biomass waste using a disruptive approach of water retention curves (WRC) for dry
659 anaerobic digestion. Bioresour. Technol. Reports 100585.
660 https://doi.org/https://doi.org/10.1016/j.biteb.2020.100585

661 Hernandez-Shek, M.A., Peultier, P., Pauss, A., Ribeiro, T., 2022. Rheological evolution of straw-cattle manure
662 (SCM) treated by dry anaerobic digestion in batch and in continuous pilot reactors. Waste Manag. 144,
663 411-420. https://doi.org/10.1016/J.WASMAN.2022.04.014

664 Holliger, C., Alves, M., Andrade, D., Angelidaki, I., Astals, S., Baier, U., Bougrier, C., Buffière, P., Carballa,
665 M., De Wilde, V., Ebertseder, F., Fernández, B., Ficara, E., Fotidis, I., Frigon, J.C., De Laclos, H.F.,
666 Ghasimi, D.S.M., Hack, G., Hartel, M., Heerenklage, J., Horvath, I.S., Jenicek, P., Koch, K., Krautwald,

667 J., Lizasoain, J., Liu, J., Mosberger, L., Nistor, M., Oechsner, H., Oliveira, J.V., Paterson, M., Pauss, A.,
668 Pommier, S., Porqueddu, I., Raposo, F., Ribeiro, T., Pfund, F.R., Strömberg, S., Torrijos, M., van Eekert,
669 M., van Lier, J., Wedwitschka, H., Wierinck, I., 2016. Towards a standardization of biomethane potential
670 tests. Water Sci. Technol. 74, 2515-2522. https://doi.org/10.2166/wst.2016.336

671 Jiang, H., Wang, S., Li, B., Feng, L., Zhai, L., Zhou, H., Li, Y., Pan, J., 2022. Anaerobic digestion of organic
672 fraction of municipal solid waste using a novel two-stage solid-liquid system. J. Clean. Prod. 370, 133521.
673 https://doi.org/10.1016/j.jclepro.2022.133521

674 Karthikeyan, O.P., Visvanathan, C., 2013. Bio-energy recovery from high-solid organic substrates by dry
675 anaerobic bio-conversion processes: A review. Rev. Environ. Sci. Biotechnol. 12, 257-284.
676 https://doi.org/10.1007/s11157-012-9304-9

677 Kim, D.H., Oh, S.E., 2011. Continuous high-solids anaerobic co-digestion of organic solid wastes under
678 mesophilic conditions. Waste Manag. 31, 1943-1948. https://doi.org/10.1016/j.wasman.2011.05.007

679 Lam, P.S., Sokhansanj, S., Bi, X., Mani, S., Lim, C.J., Womac, A.R., Hoque, M., Peng, J., JayaShankar, T.,
680 Naimi, L.J., Nayaran, S., 2008. Physical characterization of wet and dry wheat straw and switchgrass –
681 bulk and specific density. Am. Soc. Agric. Biol. Eng. 0300, 23. https://doi.org/10.13031/2013.24490

682 Li, Y., Park, S.Y., Zhu, J., 2010. Solid-state anaerobic digestion for methane production from organic waste.
683 Renew. Sustain. Energy Rev. 15, 821-826. https://doi.org/10.1016/j.rser.2010.07.042

684 Mata-Alvarez, J., Macé, S., Llabrés, P., 2000. Anaerobic digestion of organic solid wastes. An overview of
685 research achievements and perspectives. Bioresour. Technol. 74, 3-16. https://doi.org/10.1016/S0960-
686 8524(00)00023-7

687 Moreau, M., Di Miceli Raimondi, N., Le Sauze, N., Gourdon, C., Cabassud, M., 2017. A new numerical method
688 for axial dispersion characterization in microreactors. Chem. Eng. Sci. 168, 178-188.
689 https://doi.org/10.1016/j.ces.2017.04.040

690 Patinvoh, R.J., Kalantar Mehrjerdi, A., Sárvári Horváth, I., Taherzadeh, M.J., 2017. Dry fermentation of manure
691 with straw in continuous plug flow reactor: Reactor development and process stability at different loading
692 rates. Bioresour. Technol. 224, 197-205. https://doi.org/10.1016/j.biortech.2016.11.011

693 Rasouli, M., Mousavi, S.M., Azargoshasb, H., Jamialahmadi, O., Ajabshirchi, Y., 2018. CFD simulation of fluid
694 flow in a novel prototype radial mixed plug-flow reactor. J. Ind. Eng. Chem. 64, 124-133.
695 https://doi.org/10.1016/j.jiec.2018.03.008

696 Stenstrom, M.K., Rosso, D., 2003. Fundamentals of Chemical Reactor Theory. Los Angeles.

697 van Haandel, A.C., Lettinga, G., 1994. Anaerobic Sewage Treatment: A practical guide for regions with hot
698 climate. John Wiley & Sons, Chichester.

699 Veluchamy, C., Gilroyed, B.H., Kalamdhad, A.S., 2019. Process performance and biogas production optimizing
700 of mesophilic plug flow anaerobic digestion of corn silage Schematic representation of anaerobic
701 digestion of plug flow reactor in a long term experiment. https://doi.org/10.1016/j.fuel.2019.05.104

702 Wu, X., Liu, Y., Wu, H., Duan, Y., Zhang, J., 2022. Melt-processed poly (L-lactic acid) / cellulose nanocrystals
703 biocomposites for 3D printing: Improved melt processibility and inter-fuse adhesion. Compos. Sci.
704 Technol. 218, 109135. https://doi.org/10.1016/j.compscitech.2021.109135

705

706

Figure captions

Fig. 1 Schematic representation of the pilot PFR of 0.5 m3 for D-AD treatment

Fig. 2 Visual aspect of the developed 3D tracers for SRTD

Fig. 3. Experimental set-up and sampling campaign during the overall study

Fig. 4. Inlet and outlet behavior during continuous operation (IIA and IIB)

Fig. 5 (a) Recovery of the first initial tracers evenly placed in the solid bulk volume in the reactor outlet after each injection IIA **(b)** Average RDT curve for the evenly distributed tracers - IIA **(c)** Number of injections to recover each group of tracers evenly distributed in the reactor volume

Fig. 6. RTD curves for the four groups of tracers injected with the reactor fed - IIB

Fig. 7 (a) Resulted surface of the solid bed after continuous flow and distribution of tracers **(b)** Biomass injections displacement during continuous D-AD **(c)** VS content evolution under two different fresh matter (FM) load rates **(d)** Volume interpretation of each group of tracers inside the reactor

Fig. 8 (a) Biogas flow during the overall experiment **(b)** Methane content in biogas during the overall experiment and **(c)** cumulated biogas and methane during steady state - IIB

Fig. 1S Evolution of pH, buffer capacity, volatile fatty acids, and VFA/Alkalinity during the overall experiment

Video S1 Feeding system of the reactor

Video 2S Solid bed remotion layer by layer and X, Y, Z coordinates location of each 3D printing solid tracer inside the reactor

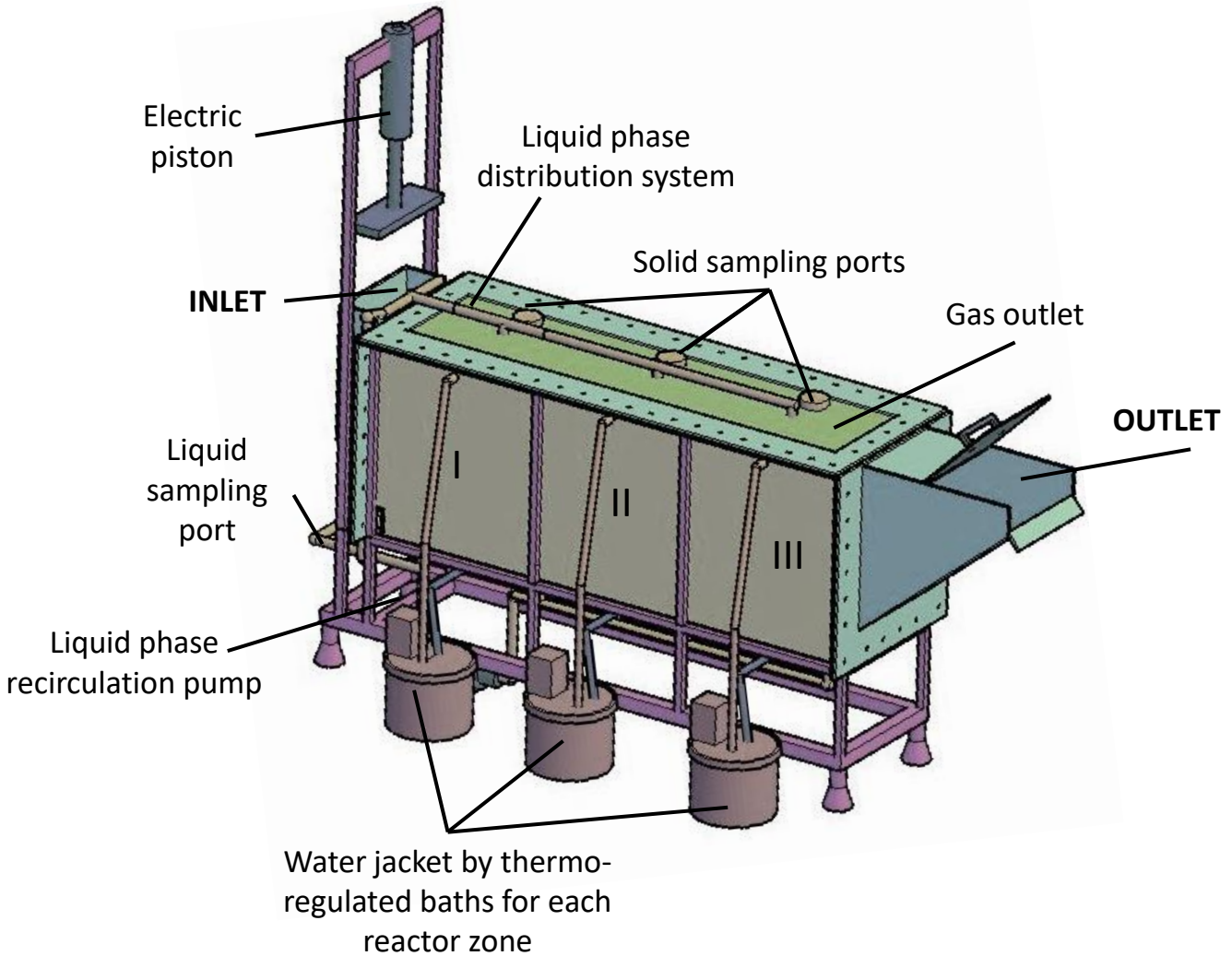
Electric piston
Liquid phase distribution system
Solid sampling ports
INLET
Gas outlet
OUTLET
Liquid sampling port
I
II
III
Liquid phase recirculation pump
Water jacket by thermo-regulated baths for each reactor zone

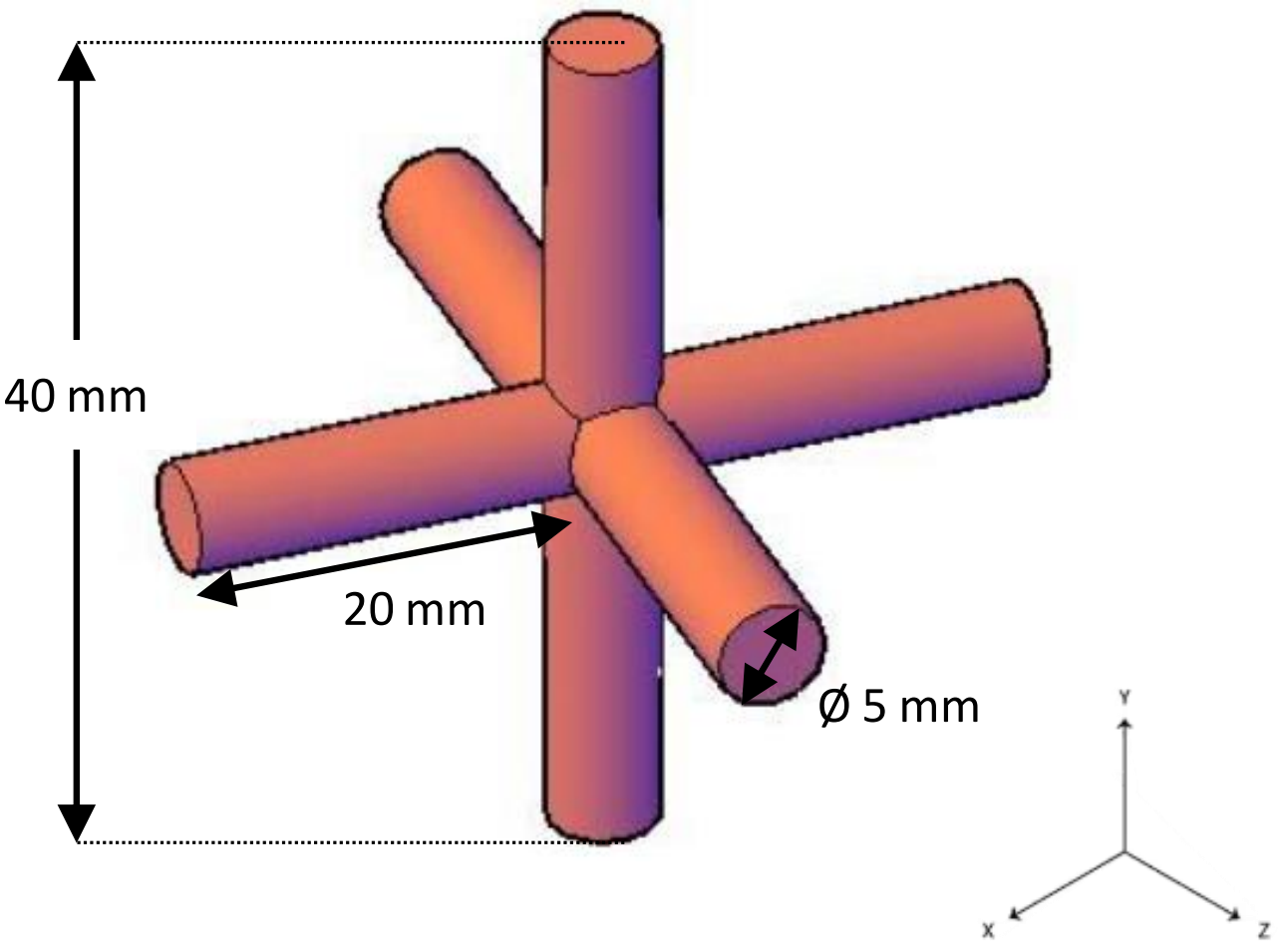
40 mm
20 mm
Ø 5 mm
Y
X
Z


Energizer

Phase I: Reactor start-up in batch

Objectives

- Launch the reactor in batch mode
- Test de reactor sealing, heating, liquid recirculation system and biogas monitoring system

The reactor was filled with substrate placing layers of tracers in an evenly manner inside the solid bed volume (11 groups of different tracer's color corresponded to a distance in the reactor length), during this phase any apport of liquid or solid matter was made, thus, not recovery of solid tracers was done

Initial axial positioning

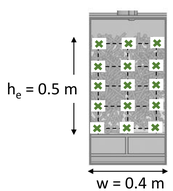

Batch launched with 222.5 kg of SCM + 80 L of tap water + 190 L of liquid inoculum

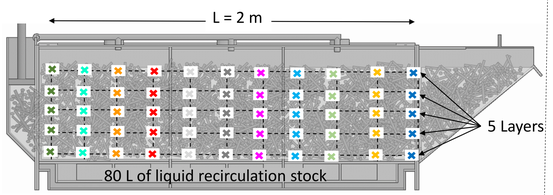

Phase I in batch ended when the biogas flow was too low (<1% of the accumulated volume)

Phase IIA: Continuous feeding

Objectives

- Study the potential of tracers to perform SRTD
- Achieve steady-state in biogas flow and outlet/inlet volume ratio
- Study the effect of the increase of solid matter and compaction over the amount of liquid phase

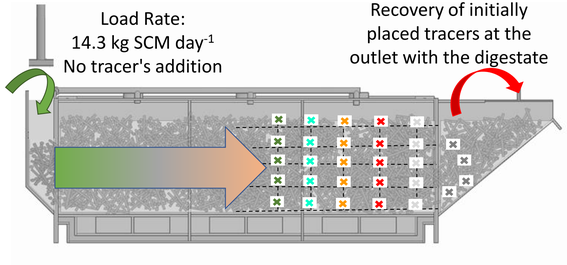

Phase IIA ended once all tracers initially placed uniformly were flushed out of the reactor by the piston effect of the feed and biogas flow achieved steady-state

Phase IIB: Continuous feeding

Objectives

- Determine the SRTD at the desired feed conditions
- Identify the solid diffusion/convection phenomena behavior using the Peclet criteria

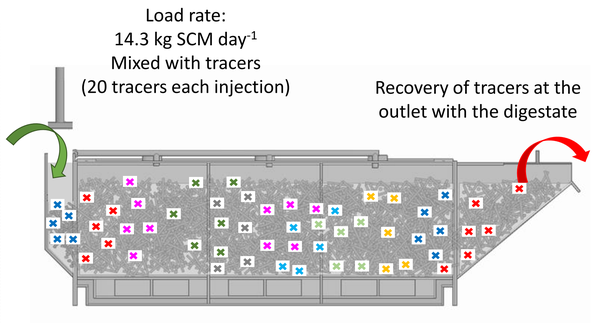

Phase IIB ended once 4 groups of tracers traversed all the distance from the reactor inlet until the outlet.

Phase III: Reactor Shut-down

Objectives

- Determine the possible injection volumetric evolution inside the reactor
- Identify short-circuits zones in the solid bed
- Solid sampling at different positions to measure the VS decrease while the solid matter advance in the reactor

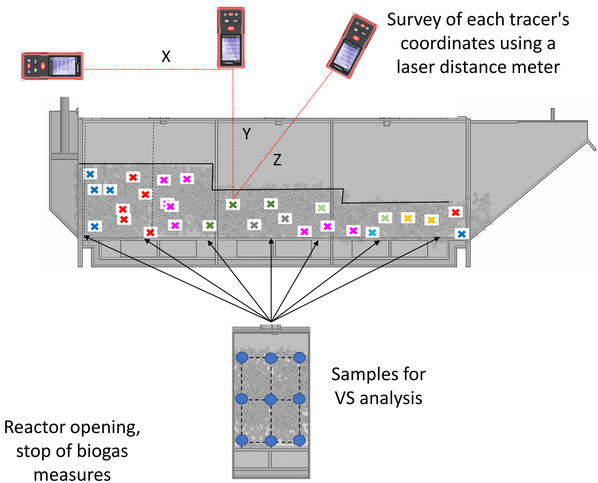

Reactor opening, stop of biogas measures

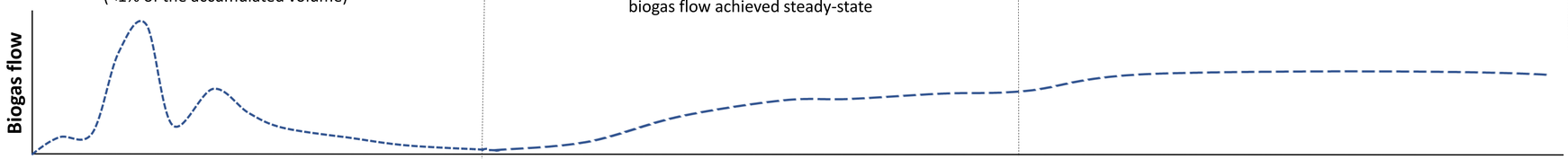

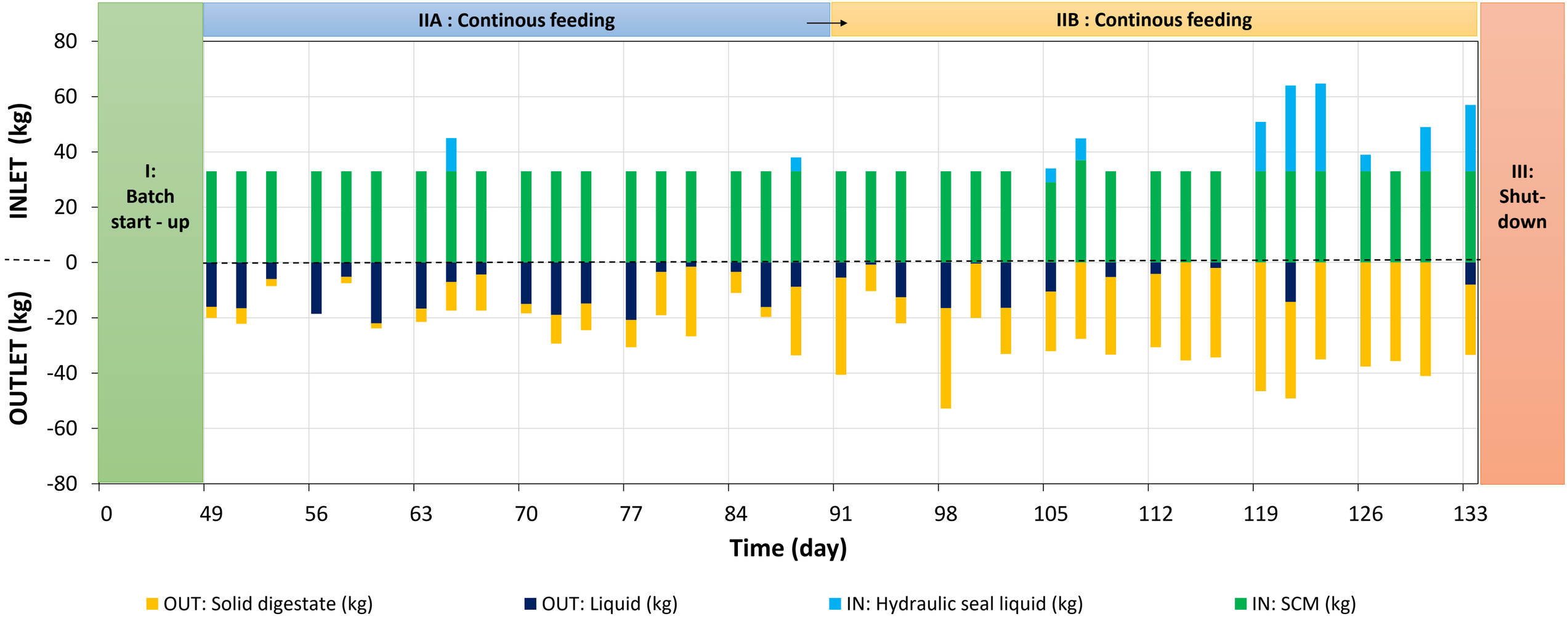
I:
Batch
start - up
IIA : Continous feeding
IIB : Continous feeding
III:
Shut-
down
INLET (kg)
OUTLET (kg)
80
60
40
20
0
-20
-40
-60
-80
0
49
56
63
70
77
84
91
98
105
112
119
126
133
Time (day)
OUT: Solid digestate (kg)
OUT: Liquid (kg)
IN: Hydraulic seal liquid (kg)
IN: SCM (kg)

(a)

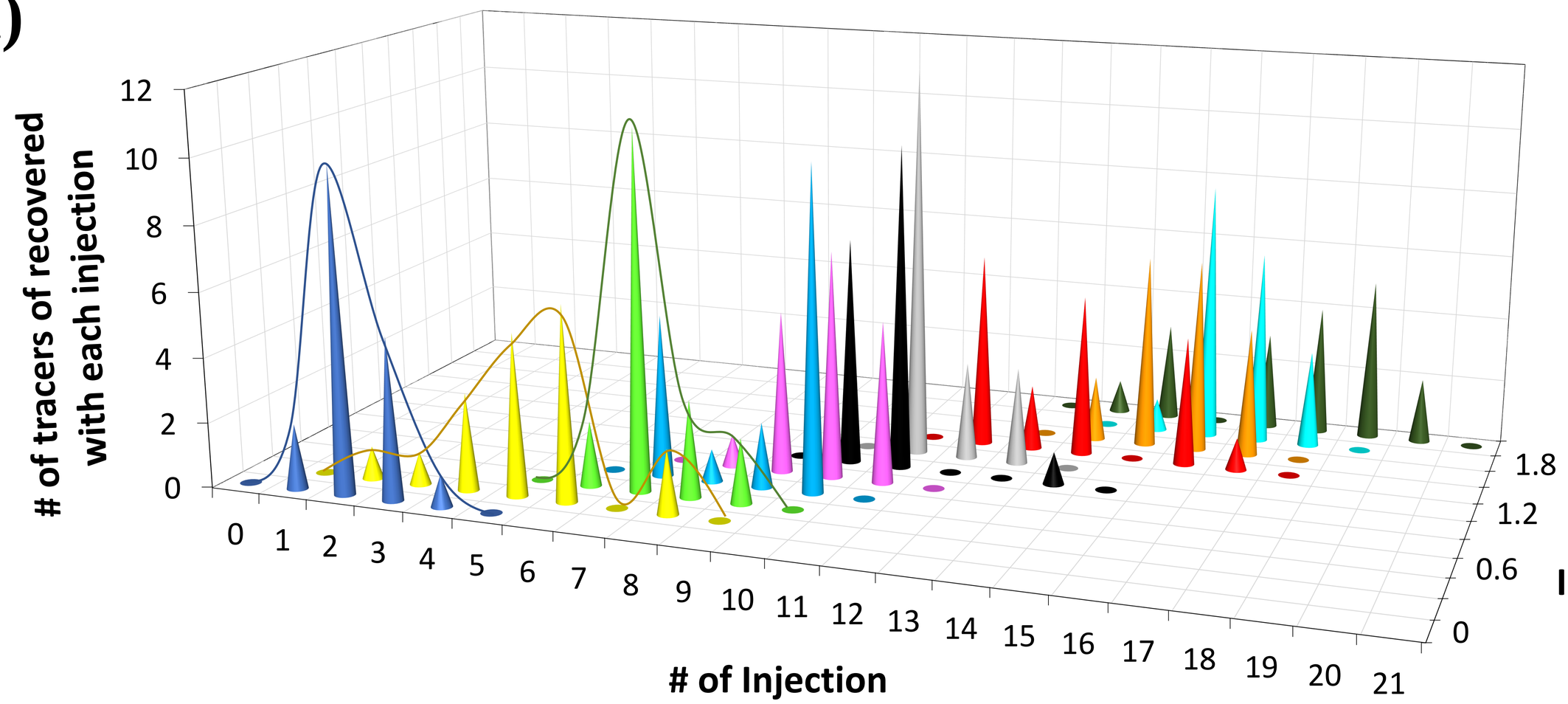
# of tracers of recovered with each injection
0
2
4
6
8
10
12
0 1 2 3 4 5 6 7 8 9 10 11 12 13 14 15 16 17 18 19 20 21
# of Injection
0
0.6
1.2
1.8
Initial distance to reach outlet (m)

(b)

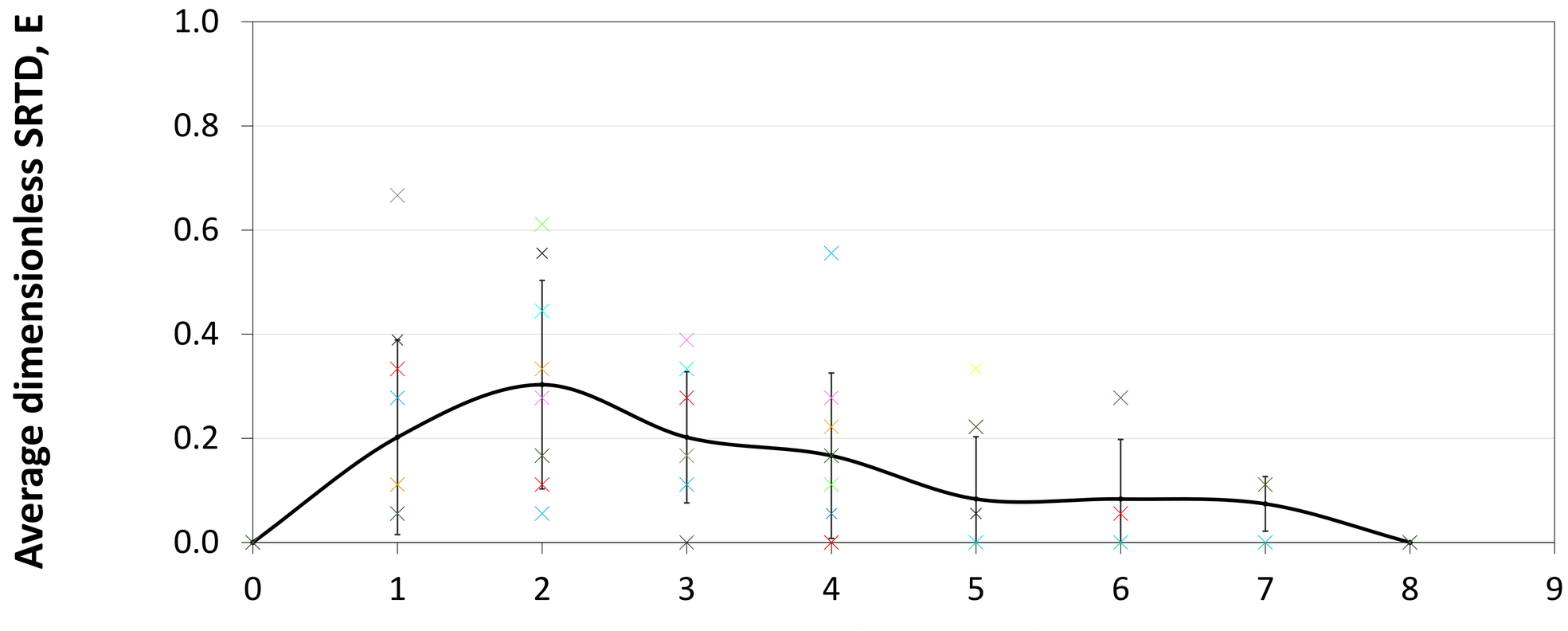
Average dimensionless SRTD, E
0.0
0.2
0.4
0.6
0.8
1.0
0 1 2 3 4 5 6 7 8 9
Dimensionless time θ

(c)

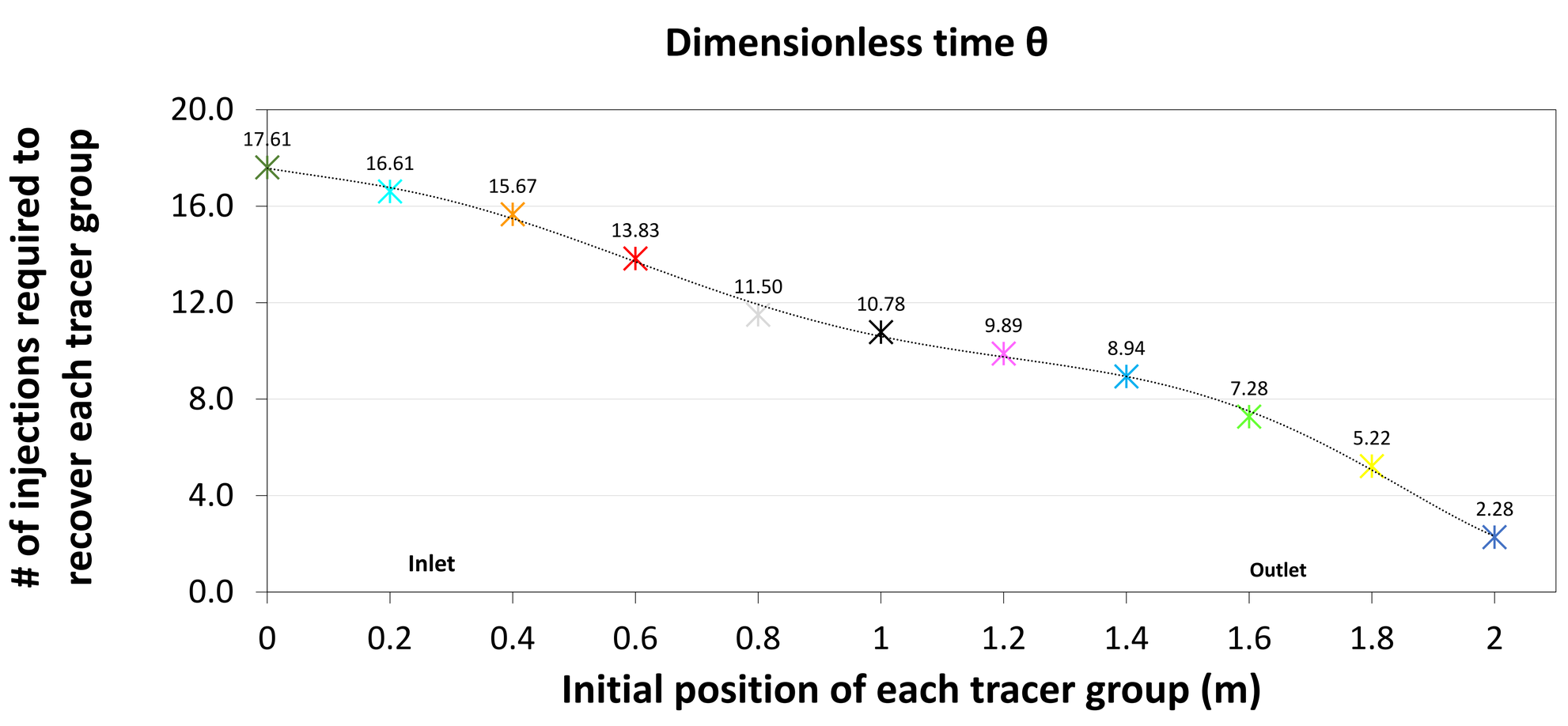
# of injections required to recover each tracer group
0.0
4.0
8.0
12.0
16.0
20.0
17.61
16.61
15.67
13.83
11.50
10.78
9.89
8.94
7.28
5.22
2.28
Inlet
Outlet
0 0.2 0.4 0.6 0.8 1 1.2 1.4 1.6 1.8 2
Initial position of each tracer group (m)

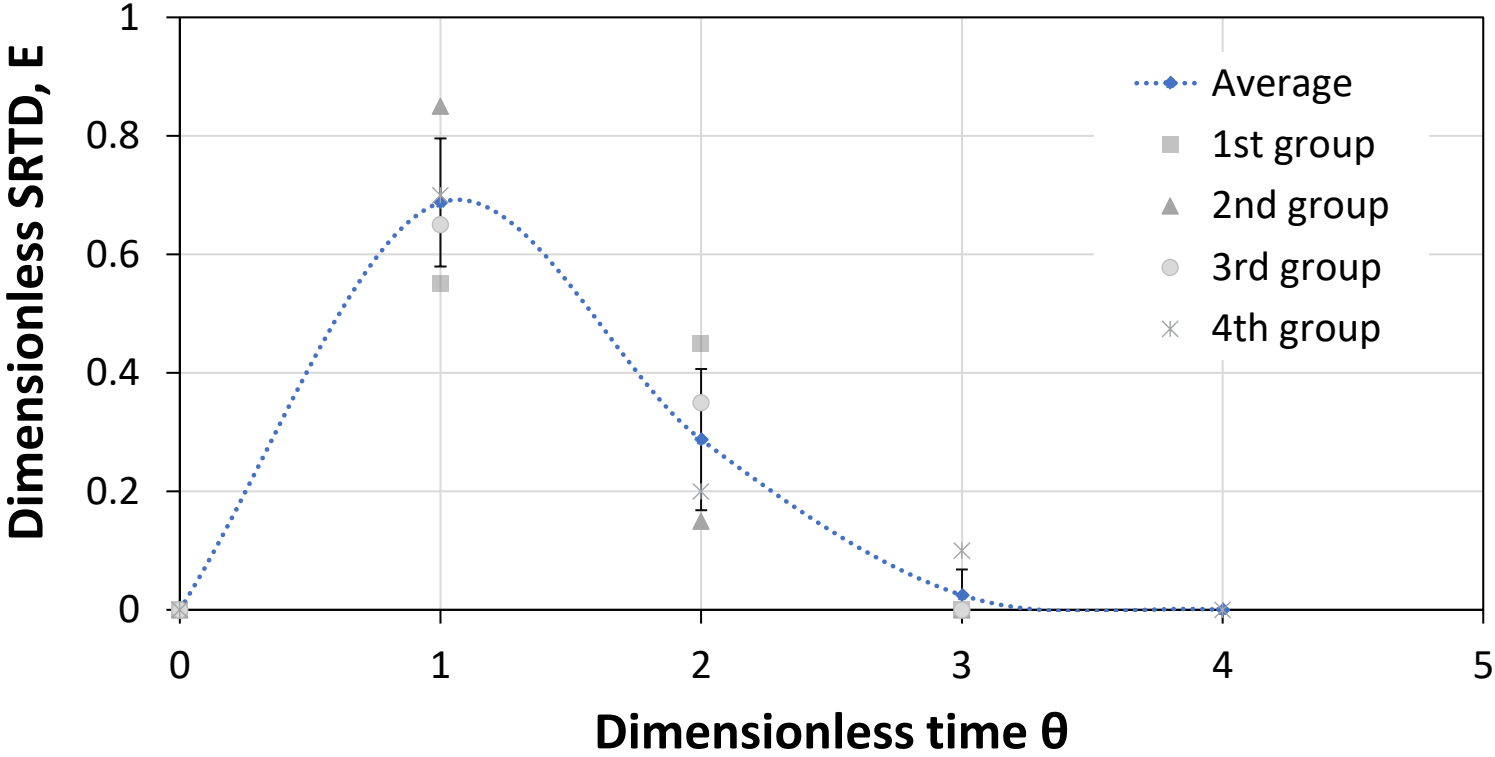
Dimensionless SRTD, E
1
0.8
0.6
0.4
0.2
0
0
1
2
3
4
5
Dimensionless time θ
Average
1st group
2nd group
3rd group
4th group

(a)

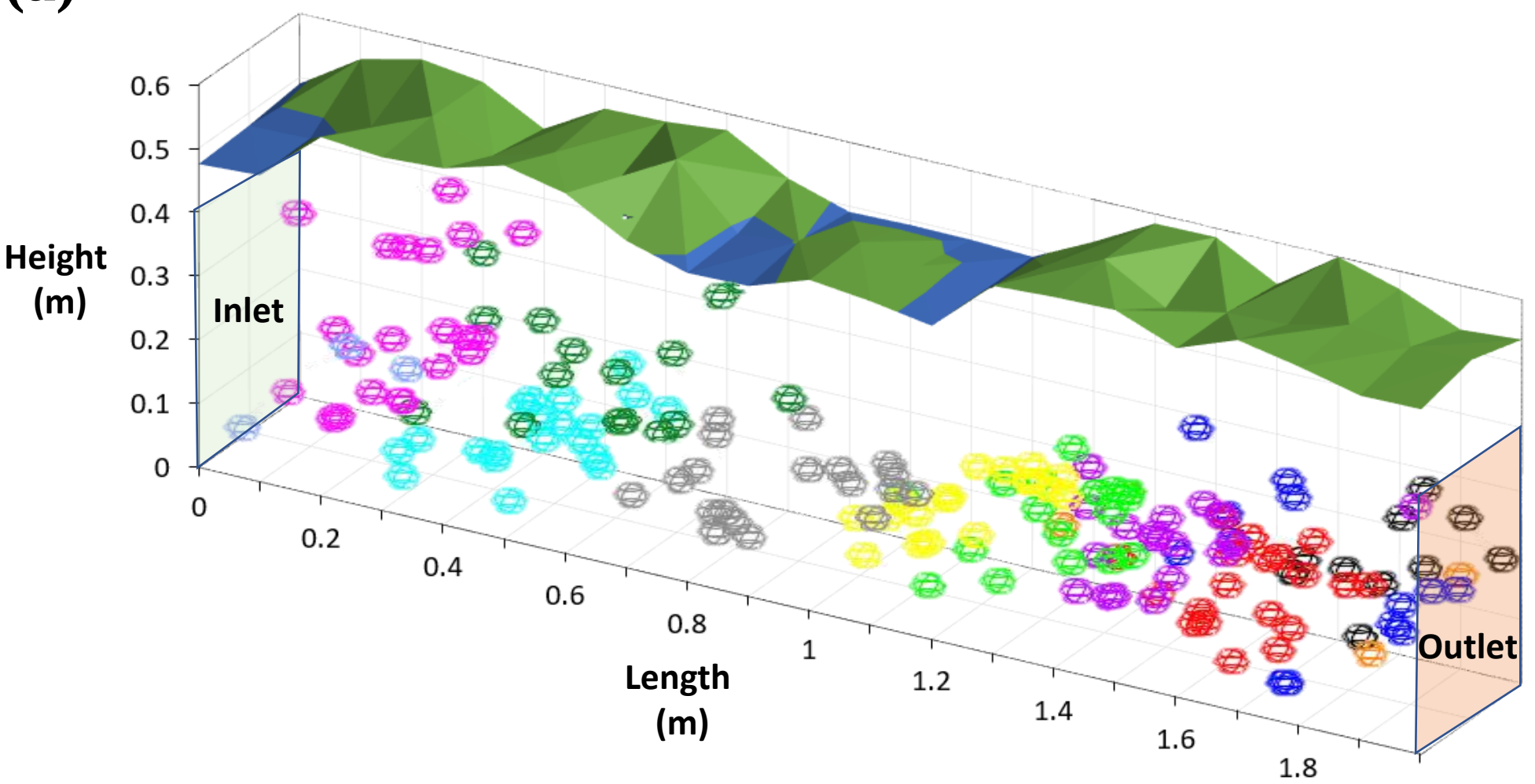
Height (m)
0.6
0.5
0.4
0.3
0.2
0.1
0
Inlet
0
0.2
0.4
0.6
0.8
1
1.2
1.4
1.6
1.8
Length (m)
Outlet

(b)

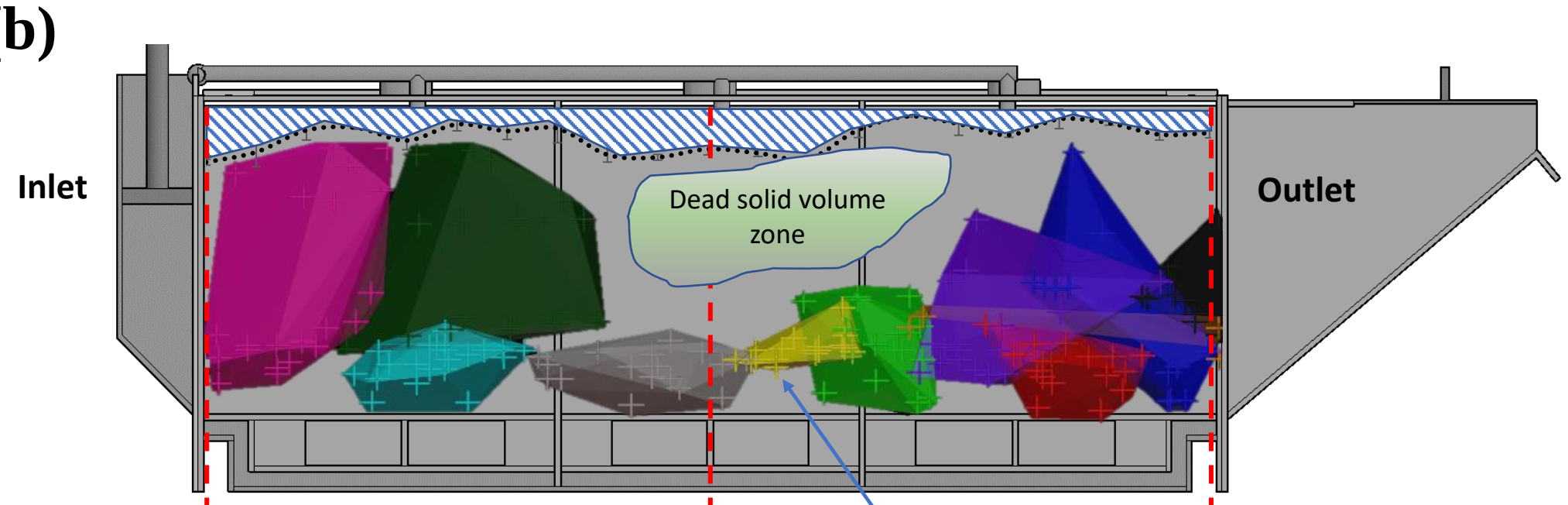
Inlet
Dead solid volume zone
Outlet
Preferential solid pathway

(c)

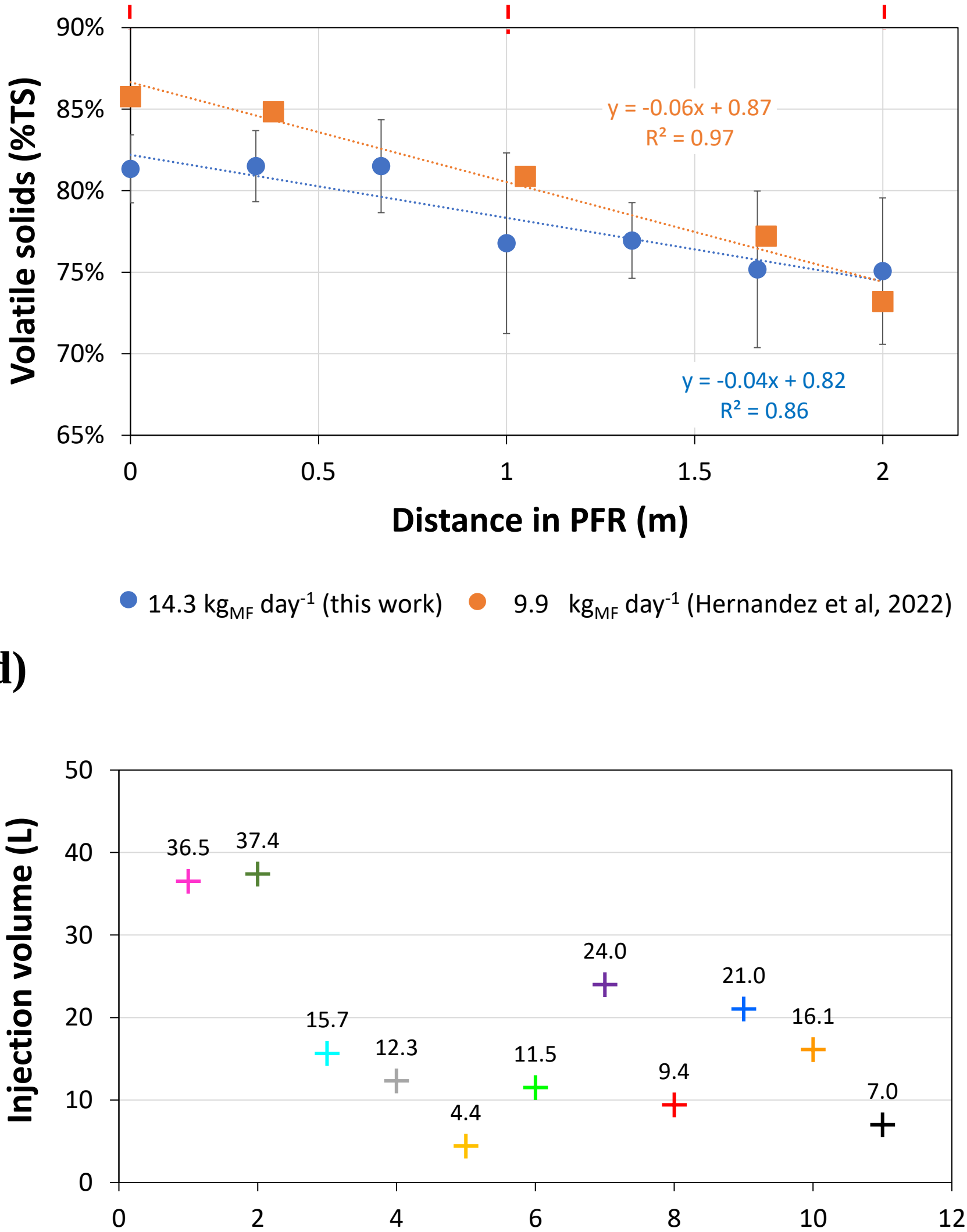
90%
85%
80%
75%
70%
65%
Volatile solids (%TS)
y = -0.06x + 0.87
R² = 0.97
y = -0.04x + 0.82
R² = 0.86
0
0.5
1
1.5
2
Distance in PFR (m)
14.3 kg$_{MF}$ day^{-1} (this work)
9.9 kg$_{MF}$ day^{-1} (Hernandez et al, 2022)

(d)

50
40
30
20
10
0
Injection volume (L)
36.5
37.4
15.7
12.3
4.4
11.5
24.0
9.4
21.0
16.1
7.0
0
2
4
6
8
10
12
# of injection

(a)

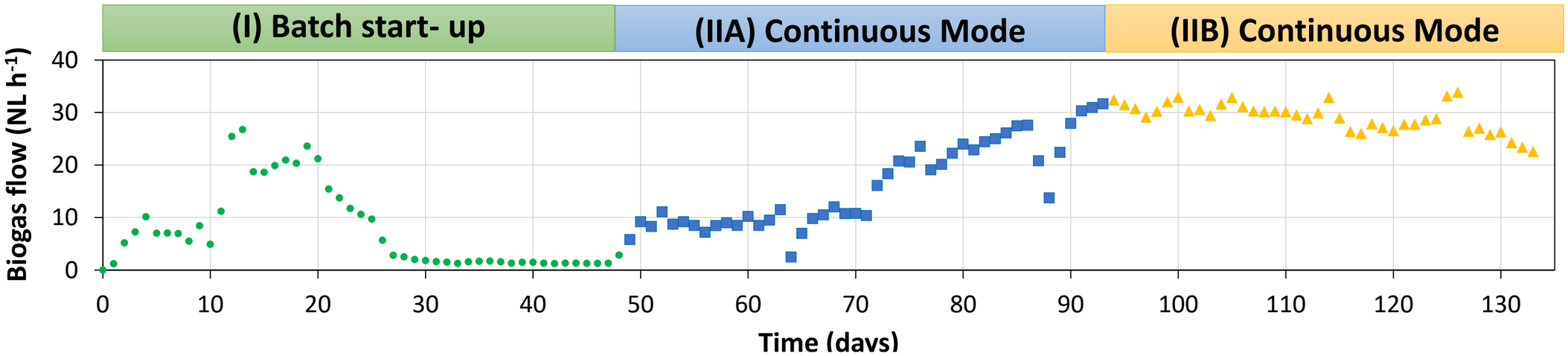
(I) Batch start- up
(IIA) Continuous Mode
(IIB) Continuous Mode
Biogas flow (NL h-1)
0
10
20
30
40
0
10
20
30
40
50
60
70
80
90
100
110
120
130
Time (days)

(b)

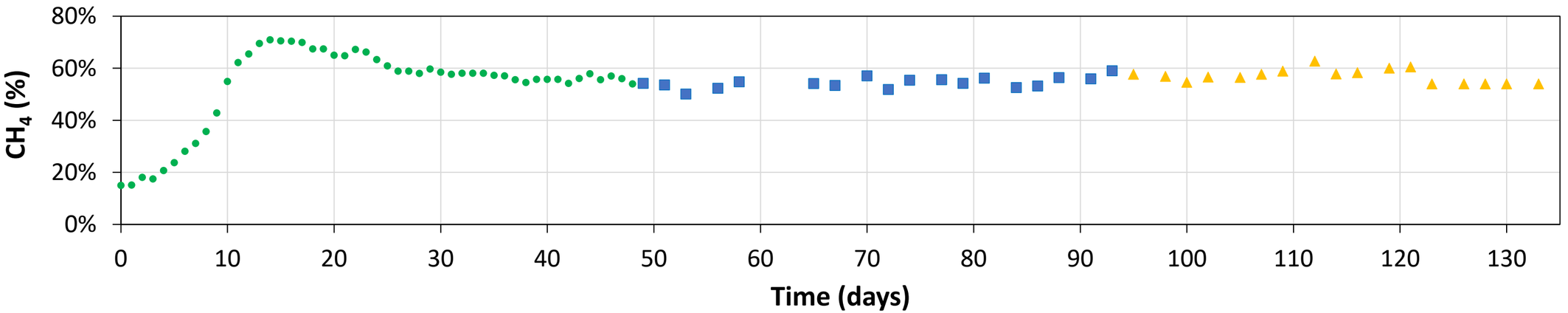
CH4 (%)
0%
20%
40%
60%
80%
0
10
20
30
40
50
60
70
80
90
100
110
120
130
Time (days)

(c)

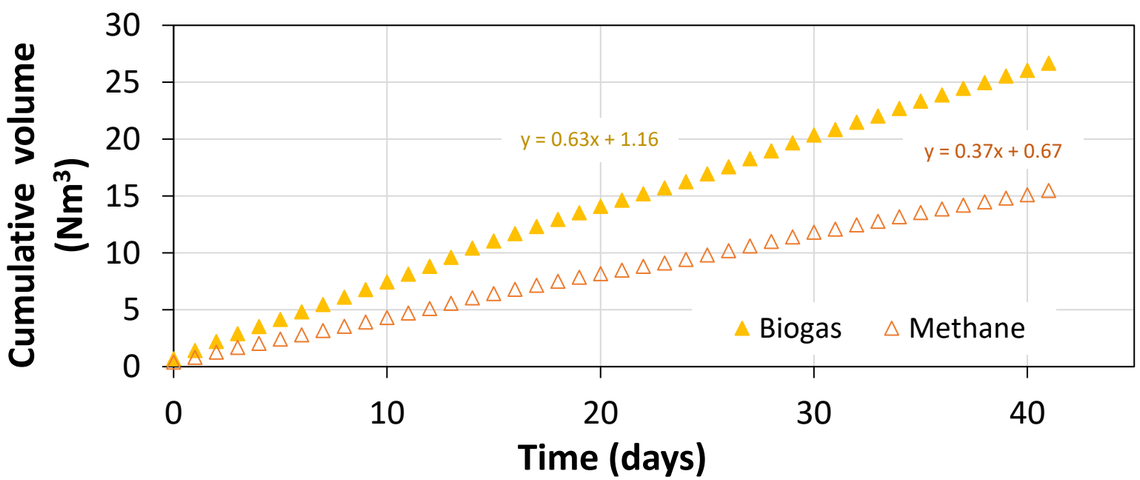
Cumulative volume (Nm3)
0
5
10
15
20
25
30
y = 0.63x + 1.16
y = 0.37x + 0.67
Biogas
Methane
0
10
20
30
40
Time (days)

Table 1. Characteristics of substrate and *inoculum* used during the experiment (standard deviation based on at least duplicate measurements).

Parameters	Straw cattle manure	*Inoculum*
TS (%)	16.6 ± 1.5	1.7 ± 0.1
VS ($\%_{TS}$)	86.5 ± 0.7	51.4 ± 0.8
pH	ND	7.71 ± 0.18
VFA (g L^{-1})	ND	0.57 ± 0.02
Alkalinity (g $CaCO_3$ L^{-1})	ND	5.15 ± 0.50
VFA/Alkalinity ratio	ND	0.113 ± 0.01
BMP (NmL CH_4 gVS_{added}^{-1})	222.13 ± 4.23	ND
Bulk density (kg m^{-3})	407.8 ± 14.1	1,002.2 ± 2.2
Solid Volume (%)	9.0 ± 0.2	ND
BMP (ml CH_4 gr^{-1}_{VS})	219.1 ± 6.5	ND

ND = Not determined; VFA = volatile fatty acids

Table 2. Experimental conditions and results of the continuous D-AD

	Parameter	Units	Value
Experimental conditions	**Substrate Load rate**	FM kg three times a week	33.30
		TS kg three times a week	5.5
		FM kg $week^{-1}$	99.90
		FM kg day^{-1}	14.27
		TS kg day^{-1}	2.37
		VS kg day^{-1}	2.04
	Time Experiment	day	41.0
	Total FM fed	kg	585.1 ± 0.2
	Total TS fed	kg	96.9 ± 1.4
	Total VS fed	kg	83.8 ± 0.6
	Digester working volume	m^3	0.4
	Organic Load Rate (OLR)	g_{VS} day^{-1} $L^{-1}_{reactor\ volume}$	5.11
Experimental results	**Retention Time**	day	29.43 ± 1.05
	Total biogas Produced	Nm^3	26.05
	Biogas Yield	Nm^3 kg_{VS}^{-1}	0.31
	Methane Yield	Nm^3 CH_4 kg_{VS}^{-1}	0.179 ± 0.009
	BMP recovery	%	78.2

FM = fresh matter

PLUG FLOW REACTOR (PFR) of 0.5 m^3 for DRY ANAEROBIC DIGESTION (D-AD)

Straw-cattle manure

Feed

Injection

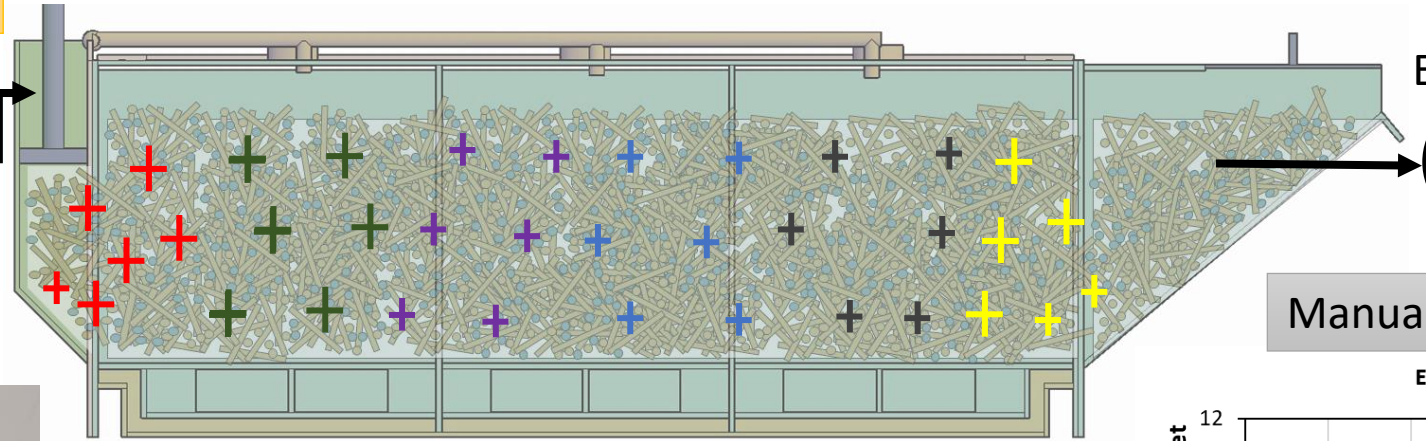

Effluent

Manual Detection

New solid 3D printed tracers

Determination of **Solid Retention Time Distribution (SRTD)**